Neural Computing and Applications (2020) 32:16025–16041
https://doi.org/10.1007/s00521-019-04604-z

BP neural network-based ABEP performance prediction for mobile Internet of Things communication systems

Lingwei Xu[1] · Jingjing Wang[1] · Han Wang[2] · T. Aaron Gulliver[3] · Khoa N. Le[4]

Received: 29 June 2019 / Accepted: 8 November 2019 / Published online: 7 December 2019

Abstract
Wireless communications play an important role in the mobile Internet of Things (IoT). For practical mobile communication systems, *N*-Nakagami fading channels are a better characterization than *N*-Rayleigh and 2-Rayleigh fading channels. The average bit error probability (ABEP) is an important factor in the performance evaluation of mobile IoT systems. In this paper, cooperative communications is used to enhance the ABEP performance of mobile IoT systems using selection combining. To compute the ABEP, the signal-to-noise ratios (SNRs) of the direct link and end-to-end link are considered. The probability density function (PDF) of these SNRs is derived, and this is used to derive the cumulative distribution function, which is used to derive closed-form ABEP expressions. The theoretical results are confirmed by Monte-Carlo simulation. The impact of fading and other parameters on the ABEP performance is examined. These results can be used to evaluate the performance of complex environments such as mobile IoT and other communication systems. To support active complex event processing in mobile IoT, it is important to predict the ABEP performance. Thus, a back-propagation (BP) neural network-based ABEP performance prediction algorithm is proposed. We use the theoretical results to generate training data. We test the extreme learning machine (ELM), linear regression (LR), support vector machine (SVM), and BP neural network methods. Compared to LR, SVM, and ELM methods, the simulation results verify that our method can consistently achieve higher ABEP performance prediction results.

Keywords Mobile Internet of Things · Mobile cooperative communication · Average bit error probability · Performance prediction · BP neural network

1 Introduction

The rapid development of the mobile Internet of Things (IoT) has led to increased interest in mobile communication systems [1–5]. A novel mobile front haul architecture was proposed in [6] for passive optical mobile networks. In [7], a two-dimensional anti-jamming mobile communication scheme was proposed which employs reinforcement learning techniques.

As a promising technology for mobile IoT, cooperative diversity has gain popularity in recent years [8, 9]. [10] investigated the secrecy outage performance of a multiple-relay-assisted non-orthogonal multiple access (NOMA) network over Nakagami-*m* fading channels. Considering MIMO-NOMA systems, [11] proposed a max–min transmit antenna selection (TAS) strategy to improve the secrecy performance. Cooperative two-way cognitive relaying was used in [12] to reduce the influence of a passive eavesdropper. Full-duplex cooperative communications were considered to provide secure communications [13]. Cooperative device-to-device communications were proposed in [14] to reduce cellular resource consumption.

To date, the research on cooperative communications has been limited to Rayleigh, Rician, and Generalized-

✉ Lingwei Xu
bh054@qust.edu.cn

Jingjing Wang
wangjingjing@qust.edu.cn

[1] Department of Information Science and Technology, Qingdao University of Science and Technology, Qingdao 266061, China

[2] College of Physical Science and Engineering, Yichun University, Yichun 336000, China

[3] Department of Electrical and Computer Engineering, University of Victoria, Victoria, BC V8W 2Y2, Canada

[4] School of Computing, Engineering and Mathematics, Western Sydney University, Kingswood, Australia

K fading channels. However, the fading in mobile cooperative communications systems is more complex and so cannot be accurately characterized by these channels [15–18]. In [19, 20], the secrecy performance of mobile cooperative networks was analyzed over 2-Rayleigh fading channels. Mobile cooperative systems over N-Rayleigh fading channels were examined in [21]. Vehicle-to-vehicle (V2V) communications over 2-Rayleigh fading channels was investigated in [22]. In [23], the secrecy outage probability (SOP) performance of wireless mobile sensor communication networks over 2-Nakagami fading channels was investigated.

In [24–26], N-Nakagami fading was considered to provide a realistic mobile channel model. N-Nakagami fading channels contain N-Rayleigh, 2-Rayleigh, Nakagami-m, and their mixtures as special cases. In particular, N-Nakagami fading is better suited to practical mobile communication environments than N-Rayleigh and 2-Rayleigh fading channels. Thus, N-Nakagami fading channels are considered here for the evaluation of mobile communication systems.

Due to the complexity of mobile IoT over N-Nakagami fading channels, secure communications is complicated. To ensure secure communications, performance changes in mobile IoT must be predicted accurately and timely. The average bit error probability (ABEP) is an important measure of mobile communication system performance, and it is important to predict the ABEP performance of mobile IoT. Because of good nonlinear prediction ability, back-propagation (BP) neural network models are very popular in engineering applications [27–29]. For complex environments such as mobile IoT, a BP neural network model is very suitable for performance prediction. To predict telecommunication customer churn, [30] used a particle classification method to optimize the BP network. Using BP neural network, [31] proposed a blind signal detection method. Weight splitting was used to improve the filtering performance of BP neural networks in [32].

However, with incremental amplify-and-forward (IAF) relaying, the ABEP performance of mobile cooperative communication systems has not previously been investigated. Further, ABEP performance prediction for mobile communication systems has not been considered. The main contributions of this paper are as follows.

1. The direct link signal-to-noise ratio (SNR) and end-to-end link SNR are derived. The probability density function (PDF) of these SNRs is derived, and the PDF is used to derive cumulative distribution function (CDF) expressions.
2. The PDF and CDF expressions are used to derive exact closed-form ABEP expressions. To verify the analysis, Monte-Carlo simulation results are compared with the theoretical ABEP. The impact of fading and other parameters on the ABEP is examined.
3. A BP neural network-based ABEP performance prediction algorithm is proposed. The ABEP theoretical results are used to generate training data. We test the extreme learning machine (ELM), linear regression (LR), support vector machines (SVM), and BP neural network methods. Compared to LR, SVM, and ELM methods, the experimental results verify that our method can consistently achieve higher ABEP performance prediction results.

This remainder of this paper is organized as follows. Section 2 presents the system model. The PDF and CDF for direct link SNR and end-to-end link SNR are obtained in Sects. 3 and 4, respectively. The ABEP is derived in Sect. 5. Based on a BP neural network, we propose a ABEP performance prediction algorithm in Sect. 6. The ABEP performance is evaluated and compared with the simulation results in Sect. 7 and Sect. 8 gives some concluding remarks.

2 System model

Figure 1 presents the mobile cooperative communication system model. This model includes a mobile source (MS) node and a mobile relay (MR) node that communicates with the mobile destination (MD) node. $G_{SD} = 1$ is the relative gain of the MS $\rightarrow$ MD link, G_{SR} is the relative gain of the MS $\rightarrow$ MR link, and G_{RD} is the relative gain of the MR $\rightarrow$ MD link. The channel coefficient $h = h_g$, $g \in \{SR,RD,SD\}$, follows an N-Nakagami distribution [24].

The total energy in the system is denoted by E. In the first time slot, MS transmits a signal x, which has mean 0 and variance 1. MR and MD receive the signals

$$r_{SD} = \sqrt{KE}h_{SD}x + n_{SD}, \quad (1)$$

$$r_{SR} = \sqrt{G_{SR}KE}h_{SR}x + n_{SR}, \quad (2)$$

where n_{SD} and n_{SR} have mean 0 and variance $N_0/2$ and K is the power allocation parameter, $0 < K \leq 1$.

The SNR of the MS $\rightarrow$ MD link is γ_{SD}. Whether MR forwards the signal to MD or not depends on the comparison between γ_{SD} and a threshold Rt. If $\gamma_{SD} > R$t, the MR will not forward the signal to MD. In this case, the SNR at MD is

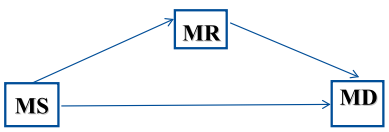

Fig. 1 The system model

$$\gamma_0 = \gamma_{\mathrm{SD}}, \tag{3}$$

where

$$\gamma_{\mathrm{SD}} = \frac{K|h_{\mathrm{SD}}|^2 E}{N_0} = K|h_{\mathrm{SD}}|^2\overline{\gamma}. \tag{4}$$

If $\gamma_{\mathrm{SD}} < R\mathrm{t}$, the MR uses AF relaying. Then MD receives the signal

$$r_{\mathrm{RD}} = \sqrt{cE}h_{\mathrm{SR}}h_{\mathrm{RD}}x + n_{\mathrm{RD}} \tag{5}$$

where n_{RD} has mean 0 and variance and $N_0/2$ and c is given by [33]

$$c = \frac{K(1-K)G_{\mathrm{SR}}G_{\mathrm{RD}}E/N_0}{1 + KG_{\mathrm{SR}}|h_{\mathrm{SR}}|^2E/N_0 + (1-K)G_{\mathrm{RD}}|h_{\mathrm{RD}}|^2E/N_0}. \tag{6}$$

The received SNR at MD is then

$$\gamma_{\mathrm{SC}} = \max(\gamma_{\mathrm{SD}}, \gamma_{\mathrm{SRD}}), \tag{7}$$

where the end-to-end link SNR is γ_{SRD}, which is given by

$$\gamma_{\mathrm{SRD}} = \frac{\gamma_{\mathrm{SR}}\gamma_{\mathrm{RD}}}{1 + \gamma_{\mathrm{SR}} + \gamma_{\mathrm{RD}}}, \tag{8}$$

$$\gamma_{\mathrm{SR}} = \frac{G_{\mathrm{SR}}K|h_{\mathrm{SR}}|^2E}{N_0} = G_{\mathrm{SR}}K|h_{\mathrm{SR}}|^2\overline{\gamma}, \tag{9}$$

$$\gamma_{\mathrm{RD}} = \frac{(1-K)G_{\mathrm{RD}}|h_{\mathrm{RD}}|^2E}{N_0} = (1-K)G_{\mathrm{RD}}|h_{\mathrm{RD}}|^2\overline{\gamma}. \tag{10}$$

For an N-Nakagami distribution, h is given by [24]

$$h = \prod_{i=1}^{N} a_i, \tag{11}$$

where a_i is a Nakagami random variable with PDF

$$f(a) = \frac{2m^m}{\Omega^m\Gamma(m)}a^{2m-1}\exp\left(-\frac{m}{\Omega}a^2\right). \tag{12}$$

The PDF of h can be expressed as

$$f(h) = \frac{2}{h\prod_{t=1}^{N}\Gamma(m_t)}G_{0,N}^{N,0}\left[h^2\prod_{t=1}^{N}\frac{m_t}{\Omega_t}\Big|\overline{m_1},\ldots,m_N\right]. \tag{13}$$

Define $y = |h_g|^2$ which has CDF and PDF

$$F(y) = \frac{1}{\prod_{t=1}^{N}\Gamma(m_t)}G_{1,N+1}^{N,1}\left[y\prod_{t=1}^{N}\frac{m_t}{\Omega_t}\Big|_{m_1,\ldots,m_N,0}^{1}\right]. \tag{14}$$

$$f(y) = \frac{1}{y\prod_{t=1}^{N}\Gamma(m_t)}G_{0,N}^{N,0}\left[y\prod_{t=1}^{N}\frac{m_t}{\Omega_t}\Big|\overline{m_1},\ldots,m_N\right]. \tag{15}$$

3 PDF and CDF of the direct link SNR

The CDF of the direct link SNR γ_{SD} is

$$F_{\gamma_{\mathrm{SD}}}(r) = \frac{1}{\prod_{i=1}^{N}\Gamma(m_i)}G_{1,N+1}^{N,1}\left[\frac{r}{\overline{\gamma_{\mathrm{SD}}}}\prod_{i=1}^{N}\frac{m_i}{\Omega_i}\Big|_{m_1,\ldots,m_N,0}^{1}\right], \tag{16}$$

where

$$\overline{\gamma_{\mathrm{SD}}} = K\overline{\gamma}, \tag{17}$$

and the corresponding PDF is

$$f_{\gamma_{\mathrm{SD}}}(r) = \frac{1}{r\prod_{i=1}^{N}\Gamma(m_i)}G_{0,N}^{N,0}\left[\frac{r}{\overline{\gamma_{\mathrm{SD}}}}\prod_{i=1}^{N}\frac{m_i}{\Omega_i}\Big|_{m_1,\ldots,m_N}^{-}\right]. \tag{18}$$

4 PDF and CDF of the end-to-end link SNR

From (8), the exact PDF and CDF of γ_{SRD} are intractable to obtain. Thus, the method in [18] is employed to approximate γ_{SRD} as

$$\gamma_{\mathrm{e}} = \frac{\gamma_{\mathrm{SR}}\gamma_{\mathrm{RD}}}{\gamma_{\mathrm{SR}} + \gamma_{\mathrm{RD}}} = \frac{1}{2}\frac{2}{\frac{1}{\gamma_{\mathrm{SR}}} + \frac{1}{\gamma_{\mathrm{RD}}}}. \tag{19}$$

From [34], we obtain that

$$\gamma_{\mathrm{e}} < \gamma_{\mathrm{up}} = \min(\gamma_{\mathrm{SR}}, \gamma_{\mathrm{RD}}), \tag{20}$$

so, the CDF is lower bounded as

$$F_{\gamma_{\mathrm{SRD}}}(r) > F_{\gamma_{\mathrm{up}}}(r). \tag{21}$$

The CDF of γ_{up} is

$$\begin{aligned}
F_{\gamma_{\mathrm{up}}}(r) &= 1 - \left(1 - \frac{1}{\prod_{t=1}^{N}\Gamma(m_t)}G_{1,N+1}^{N,1}\left[\frac{r}{\overline{\gamma_{\mathrm{SR}}}}\prod_{t=1}^{N}\frac{m_t}{\Omega_t}\Big|_{m_1,\ldots,m_N,0}^{1}\right]\right) \\
&\quad\times\left(1 - \frac{1}{\prod_{tt=1}^{N}\Gamma(m_{tt})}G_{1,N+1}^{N,1}\left[\frac{r}{\overline{\gamma_{\mathrm{RD}}}}\prod_{tt=1}^{N}\frac{m_{tt}}{\Omega_{tt}}\Big|_{m_1,\ldots,m_N,0}^{1}\right]\right) \\
&= \frac{1}{\prod_{t=1}^{N}\Gamma(m_t)}G_{1,N+1}^{N,1}\left[\frac{r}{\overline{\gamma_{\mathrm{SR}}}}\prod_{t=1}^{N}\frac{m_t}{\Omega_t}\Big|_{m_1,\ldots,m_N,0}^{1}\right] \\
&\quad+\frac{1}{\prod_{tt=1}^{N}\Gamma(m_{tt})}G_{1,N+1}^{N,1}\left[\frac{r}{\overline{\gamma_{\mathrm{RD}}}}\prod_{tt=1}^{N}\frac{m_{tt}}{\Omega_{tt}}\Big|_{m_1,\ldots,m_N,0}^{1}\right] \\
&\quad-\frac{1}{\prod_{t=1}^{N}\Gamma(m_t)\prod_{tt=1}^{N}\Gamma(m_{tt})}G_{1,N+1}^{N,1}\left[\frac{r}{\overline{\gamma_{\mathrm{SR}}}}\prod_{t=1}^{N}\frac{m_t}{\Omega_t}\Big|_{m_1,\ldots,m_N,0}^{1}\right] \\
&\quad\times G_{1,N+1}^{N,1}\left[\frac{r}{\overline{\gamma_{\mathrm{RD}}}}\prod_{tt=1}^{N}\frac{m_{tt}}{\Omega_{tt}}\Big|_{m_1,\ldots,m_N,0}^{1}\right]
\end{aligned} \tag{22}$$

and the corresponding PDF is

$$f_{\gamma_{\text{up}}}(r) = \frac{1}{r\prod_{t=1}^{N}\Gamma(m_t)} G_{0,N}^{N,0}\left[\frac{r}{\overline{\gamma_{\text{SR}}}}\prod_{t=1}^{N}\frac{m_t}{\Omega_t}\Big|_{m_1,\ldots,m_N}^{-}\right] + \frac{1}{r\prod_{tt=1}^{N}\Gamma(m_{tt})} G_{0,N}^{N,0}\left[\frac{r}{\overline{\gamma_{\text{RD}}}}\prod_{tt=1}^{N}\frac{m_{tt}}{\Omega_{tt}}\Big|_{m_1,\ldots,m_N}^{-}\right] - \frac{1}{r\prod_{t=1}^{N}\Gamma(m_t)\prod_{tt=1}^{N}\Gamma(m_{tt})} \times \left(\begin{array}{l} G_{0,N}^{N,0}\left[\frac{r}{\overline{\gamma_{\text{SR}}}}\prod_{t=1}^{N}\frac{m_t}{\Omega_t}\Big|_{m_1,\ldots,m_N}^{-}\right] G_{1,N+1}^{N,1}\left[\frac{r}{\overline{\gamma_{\text{RD}}}}\prod_{tt=1}^{N}\frac{m_{tt}}{\Omega_{tt}}\Big|_{m_1,\ldots,m_N,0}^{1}\right] \\ +G_{1,N+1}^{N,1}\left[\frac{r}{\overline{\gamma_{\text{SR}}}}\prod_{t=1}^{N}\frac{m_t}{\Omega_t}\Big|_{m_1,\ldots,m_N,0}^{1}\right] G_{0,N}^{N,0}\left[\frac{r}{\overline{\gamma_{\text{RD}}}}\prod_{tt=1}^{N}\frac{m_{tt}}{\Omega_{tt}}\Big|_{m_1,\ldots,m_N}^{-}\right] \end{array}\right). \tag{23}$$

5 ABEP performance

The ABEP can be expressed as [35]

$$P(\text{e}) = \Pr(\gamma_{\text{SD}} < R\text{t}) \times P_{\text{div}}(\text{e}) + \Pr(\gamma_{\text{SD}} \geq R\text{t}) \times P_{\text{direct}}(\text{e}), \tag{24}$$

where the error probability of MD is $P_{\text{div}}(\text{e})$, when MR forwards the signal to MD and $P_{\text{direct}}(\text{e})$ is the corresponding error probability given that the MR does not forward the signal to MD. We have

$$\Pr(\gamma_{SD} < Rt) = F_{\gamma_{SD}}(Rt) = \frac{1}{\prod_{i=1}^{N}\Gamma(m_i)} G_{1,N+1}^{N,1}\left[\frac{Rt}{\overline{\gamma_{SD}}}\prod_{i=1}^{N}\frac{m_i}{\Omega_i}\Big|_{m_1,\ldots,m_N,0}^{1}\right], \tag{25}$$

$$\Pr(\gamma_{\text{SD}} \geq R\text{t}) = 1 - \Pr(\gamma_{\text{SD}} < R\text{t}) = 1 - \frac{1}{\prod_{i=1}^{N}\Gamma(m_i)} G_{1,N+1}^{N,1}\left[\frac{R\text{t}}{\overline{\gamma_{\text{SD}}}}\prod_{i=1}^{N}\frac{m_i}{\Omega_i}\Big|_{m_1,\ldots,m_N,0}^{1}\right], \tag{26}$$

and

$$P_{\text{direct}}(\text{e}) = \int_0^{\infty} P_{\text{direct}}(\text{e}|r) f_{\gamma_{\text{SD}}}(r|\gamma_{\text{SD}} \geq R\text{t}) dr, \tag{27}$$

where

$$P_{\text{direct}}(\text{e}|r) = a \times \text{erfc}(\sqrt{br}). \tag{28}$$

The type of modulation decides the constants a and b, e.g., $a = 0.5$ and $b = 1$ for BPSK, and $a = 0.5$ and $b = 0.5$ for QPSK. Further

$$f_{\gamma_{\text{SD}}}(r|\gamma_{\text{SD}} \geq R\text{t}) = \begin{cases} 0, & r \leq R\text{t} \\ \dfrac{\frac{1}{r\prod_{i=1}^{N}\Gamma(m_i)} G_{0,N}^{N,0}\left[\frac{r}{\overline{\gamma_{\text{SD}}}}\prod_{i=1}^{N}\frac{m_i}{\Omega_i}\Big|_{m_1,\ldots,m_N}^{-}\right]}{1 - \frac{1}{\prod_{i=1}^{N}\Gamma(m_i)} G_{1,N+1}^{N,1}\left[\frac{R\text{t}}{\overline{\gamma_{\text{SD}}}}\prod_{i=1}^{N}\frac{m_i}{\Omega_i}\Big|_{m_1,\ldots,m_N,0}^{1}\right]}, & r > R\text{t} \end{cases} = \begin{cases} 0, & r \leq R\text{t} \\ \dfrac{\frac{1}{r} G_{0,N}^{N,0}\left[\frac{r}{\overline{\gamma_{\text{SD}}}}\prod_{i=1}^{N}\frac{m_i}{\Omega_i}\Big|_{m_1,\ldots,m_N}^{-}\right]}{\prod_{i=1}^{N}\Gamma(m_i) - G_{1,N+1}^{N,1}\left[\frac{R\text{t}}{\overline{\gamma_{\text{SD}}}}\prod_{i=1}^{N}\frac{m_i}{\Omega_i}\Big|_{m_1,\ldots,m_N,0}^{1}\right]}, & r > R\text{t}. \end{cases} \tag{29}$$

Combining (28) and (29), we obtain

$$\begin{aligned} P_{\text{direct}}(\text{e}) &= \frac{a}{\prod_{i=1}^{N}\Gamma(m_i) - G_{1,N+1}^{N,1}\left[\frac{R\text{t}}{\overline{\gamma_{\text{SD}}}}\prod_{i=1}^{N}\frac{m_i}{\Omega_i}\Big|_{m_1,\ldots,m_N,0}^{1}\right]} \times \int_{Rt}^{\infty} \text{erfc}(\sqrt{br}) \frac{1}{r} G_{0,N}^{N,0}\left[\frac{r}{\overline{\gamma_{\text{SD}}}}\prod_{i=1}^{N}\frac{m_i}{\Omega_i}\Big|_{m_1,\ldots,m_N}^{-}\right] dr \\ &= \frac{a}{\prod_{i=1}^{N}\Gamma(m_i) - G_{1,N+1}^{N,1}\left[\frac{R\text{t}}{\overline{\gamma_{\text{SD}}}}\prod_{i=1}^{N}\frac{m_i}{\Omega_i}\Big|_{m_1,\ldots,m_N,0}^{1}\right]} \times \left[\int_0^{\infty} \text{erfc}(\sqrt{br}) \frac{1}{r} G_{0,N}^{N,0}\left[\frac{r}{\overline{\gamma_{\text{SD}}}}\prod_{i=1}^{N}\frac{m_i}{\Omega_i}\Big|_{m_1,\ldots,m_N}^{-}\right] dr - \int_0^{Rt} \text{erfc}(\sqrt{br}) \frac{1}{r} G_{0,N}^{N,0}\left[\frac{r}{\overline{\gamma_{\text{SD}}}}\prod_{i=1}^{N}\frac{m_i}{\Omega_i}\Big|_{m_1,\ldots,m_N}^{-}\right] dr\right] \\ &= \frac{a}{\prod_{i=1}^{N}\Gamma(m_i) - G_{1,N+1}^{N,1}\left[\frac{R\text{t}}{\overline{\gamma_{\text{SD}}}}\prod_{i=1}^{N}\frac{m_i}{\Omega_i}\Big|_{m_1,\ldots,m_N,0}^{1}\right]} [V_1 - V_2], \end{aligned} \tag{30}$$

where

$$\begin{aligned} V_1 &= \int_0^{\infty} erfc(\sqrt{br}) \frac{1}{r} G_{0,N}^{N,0}\left[\frac{r}{\overline{\gamma_{SD}}}\prod_{i=1}^{N}\frac{m_i}{\Omega_i}\Big|_{m_1,\ldots,m_N}^{-}\right] dr \\ &= \frac{1}{\sqrt{\pi}} \int_0^{\infty} r^{-1} G_{1,2}^{2,0}\left(br\Big|_{0,\frac{1}{2}}^{1}\right) G_{0,N}^{N,0}\left[\frac{r}{\overline{\gamma_{SD}}}\prod_{i=1}^{N}\frac{m_i}{\Omega_i}\Big|_{m_1,\ldots,m_N}^{-}\right] dr. \end{aligned} \tag{31}$$

Using the results in [36], we obtain

$$V_1 = \frac{1}{\sqrt{\pi}\prod_{i=1}^{N}\Gamma(m_i)} G_{2,N+1}^{N,2}\left[\frac{1}{b\overline{\gamma_{\text{SD}}}}\prod_{i=1}^{N}\frac{m_i}{\Omega_i}\Big|_{m_1,\ldots,m_N,0}^{1,\frac{1}{2}}\right]. \tag{32}$$

Further, V_2 is given by

$$v_2 = \int_0^{R\mathrm{t}} \mathrm{erfc}(\sqrt{br})\frac{1}{r}G_{0,N}^{N,0}\left[\frac{r}{\overline{\gamma}_{\mathrm{SD}}}\prod_{i=1}^{N}\frac{m_i}{\Omega_i}\Big|_{m_1,\ldots,m_N}^{-}\right]\mathrm{d}r$$
$$= \frac{1}{\sqrt{\pi}}\int_0^{R\mathrm{t}} r^{-1}G_{1,2}^{2,0}\left(br\Big|_{0,\frac{1}{2}}^{1}\right)G_{0,N}^{N,0}\left[\frac{r}{\overline{\gamma}_{\mathrm{SD}}}\prod_{i=1}^{N}\frac{m_i}{\Omega_i}\Big|_{m_1,\ldots,m_N}^{-}\right]\mathrm{d}r. \tag{33}$$

A closed-form solution to (33) is difficult to obtain. Thus, using Meijer's G-function [37]

$$G_{p,q}^{m,n}\left[z\Big|_{b_1,\ldots,b_q}^{a_1,\ldots,a_p}\right] = \sum_{h=1}^{m}\frac{\prod_{i=1}^{m}\Gamma(b_i-b_h)\prod_{i=1}^{n}\Gamma(1+b_h-a_i)}{\prod_{i=n+1}^{p}\Gamma(a_i-b_h)\prod_{i=m+1}^{q}\Gamma(1+b_h-b_i)}z^{b_h} \times {}_pF_{q-1}\left(1+b_h-a_1,\ldots,1+b_h-a_p;1+b_h-b_1,\ldots,1+b_h-b_q;(-1)^{p-m-n}z\right). \tag{34}$$

$${}_pF_q(\alpha_1,\alpha_2,\ldots,\alpha_p;\beta_1,\beta_2,\ldots,\beta_q;z) = \sum_{k=0}^{\infty}\frac{(\alpha_1)_k(\alpha_2)_k\cdots(\alpha_p)_k}{(\beta_1)_k(\beta_2)_k\cdots(\beta_q)_k}\frac{z^k}{k!}. \tag{35}$$

$$(x)_k = \prod_{t=0}^{k-1}(x+t),(x)_0 = 1, \tag{36}$$

whichgives

$$G_{1,2}^{2,0}\left[br\Big|_{0,\frac{1}{2}}^{1}\right] = \Gamma(1/2){}_1F_1\left(0;1,\frac{1}{2};-br\right) + \frac{\Gamma(-1/2)}{\Gamma(1/2)}(br)^{\frac{1}{2}}{}_1F_1\left(\frac{1}{2};\frac{3}{2},1;-br\right) = \sqrt{\pi} + \frac{\Gamma(-1/2)}{\sqrt{\pi}}\sum_{k=0}^{\infty}\frac{(1/2)_k(-1)^k(b)^{k+\frac{1}{2}}}{(3/2)_k k!}r^{k+\frac{1}{2}} \tag{37}$$

so that

$$V_2 = \int_0^{R\mathrm{t}} r^{-1}G_{0,N}^{N,0}\left[\frac{r}{\overline{\gamma}_{\mathrm{SD}}}\prod_{i=1}^{N}\frac{m_i}{\Omega_i}|\overline{m_1},\ldots,m_N\right]\mathrm{d}r + \frac{\Gamma(-1/2)}{\pi}\sum_{k=0}^{\infty}\frac{(1/2)_k(-1)^k(b)^{k+\frac{1}{2}}}{(3/2)_k(k!)^2} \times \int_0^{R\mathrm{t}} r^{k-\frac{1}{2}}G_{0,N}^{N,0}\left[\frac{r}{\overline{\gamma}_{\mathrm{SD}}}\prod_{i=1}^{N}\frac{m_i}{\Omega_i}|\overline{m_1},\ldots,m_N\right]\mathrm{d}r \tag{38}$$
$$= G_{1,N+1}^{N,1}\left[\frac{R_{\mathrm{t}}}{\overline{\gamma}_{\mathrm{SD}}}\prod_{i=1}^{N}\frac{m_i}{\Omega_i}\Big|_{m_1,\ldots,m_N,0}^{1}\right] + A\sum_{k=0}^{\infty}BG_{1,N+1}^{N,1}\left[\frac{R_{\mathrm{t}}}{\overline{\gamma}_{\mathrm{SD}}}\prod_{i=1}^{N}\frac{m_i}{\Omega_i}\Big|_{m_1,\ldots,m_N,-k-\frac{1}{2}}^{\frac{1}{2}-k}\right].$$

$$A = \frac{\Gamma(-1/2)}{\pi}, \quad B = \frac{(1/2)_k(-1)^k(b)^{k+\frac{1}{2}}}{(3/2)_k(k!)^2}. \tag{39}$$

We have

$$P_{\mathrm{div}}(e) = a\int_0^{\infty}\mathrm{erfc}\left(\sqrt{br}\right)f_{\gamma_{\mathrm{SC}}}(r|\gamma_{\mathrm{SD}}<R\mathrm{t})\mathrm{d}r, \tag{40}$$

where

$$f_{\gamma_{\mathrm{SC}}}(r|\gamma_{\mathrm{SD}}<R\mathrm{t}) = \begin{cases}\frac{1}{F_{\gamma_{\mathrm{SD}}}(R\mathrm{t})}\left(f_{\gamma_{\mathrm{SD}}}(r)F_{\gamma_{\mathrm{up}}}(r)+F_{\gamma_{\mathrm{SD}}}(r)f_{\gamma_{\mathrm{up}}}(r)\right), r\le R\mathrm{t}\\ f_{\gamma_{\mathrm{up}}}(r), \quad r>R\mathrm{t}\end{cases}. \tag{41}$$

Combining (32) and (33) gives

$$P_{\mathrm{div}}(\mathrm{e}) = a\left[\frac{1}{F_{\gamma_{\mathrm{SD}}}(R\mathrm{t})}(V_3+V_4)+V_5\right], \tag{42}$$

where

$$V_3 = \int_0^{R\mathrm{t}}\mathrm{erfc}(\sqrt{br})f_{\gamma_{\mathrm{SD}}}(r)F_{\gamma_{\mathrm{up}}}(r)\mathrm{d}r$$
$$= \frac{1}{\prod_{t=1}^{N}\Gamma(m_t)}\int_0^{R\mathrm{t}}\mathrm{erfc}(\sqrt{br})f_{\gamma_{\mathrm{SD}}}(r)G_{1,N+1}^{N,1} \times\left[\frac{r}{\overline{\gamma}_{\mathrm{SR}}}\prod_{t=1}^{N}\frac{m_t}{\Omega_t}\Big|_{m_1,\ldots,m_N,0}^{1}\right]\mathrm{d}r$$
$$+\frac{1}{\prod_{tt=1}^{N}\Gamma(m_{tt})}\int_0^{R\mathrm{t}}\mathrm{erfc}(\sqrt{br})f_{\gamma_{\mathrm{SD}}}(r)G_{1,N+1}^{N,1} \times\left[\frac{r}{\overline{\gamma}_{\mathrm{RD}}}\prod_{tt=1}^{N}\frac{m_{tt}}{\Omega_{tt}}\Big|_{m_1,\ldots\infty,m_N,0}^{1}\right]\mathrm{d}r$$
$$-\frac{1}{\prod_{t=1}^{N}\Gamma(m_t)\prod_{tt=1}^{N}\Gamma(m_{tt})}\int_0^{R\mathrm{t}}\mathrm{erfc}(\sqrt{br})f_{\gamma_{\mathrm{SD}}}(r)G_{1,N+1}^{N,1} \times\left[\frac{r}{\overline{\gamma}_{\mathrm{SR}}}\prod_{t=1}^{N}\frac{m_t}{\Omega_t}\Big|_{m_1,\ldots,m_N,0}^{1}\right] \times G_{1,N+1}^{N,1}\left[\frac{r}{\overline{\gamma}_{\mathrm{RD}}}\prod_{tt=1}^{N}\frac{m_{tt}}{\Omega_{tt}}\Big|_{m_1,\ldots,m_N,0}^{1}\right]\mathrm{d}r$$
$$= \mathrm{VA}_1+\mathrm{VA}_2-\mathrm{VA}_3. \tag{43}$$

$$
\begin{aligned}
V_4 &= \int_0^{Rt} \operatorname{erfc}(\sqrt{br}) F_{\gamma_{\mathrm{SD}}}(r) f_{\gamma_{\mathrm{up}}}(r)\mathrm{d}r \\
&= \frac{1}{\prod_{t=1}^{N}\Gamma(m_t)} \int_0^{Rt} \operatorname{erfc}(\sqrt{br}) F_{\gamma_{\mathrm{SD}}}(r) \frac{1}{r} G_{0,N}^{N,0} \\
&\quad \times \left[\frac{r}{\overline{\gamma}_{\mathrm{SR}}} \prod_{t=1}^{N} \frac{m_t}{\Omega_t} \Big|_{m_1,\ldots,m_N}^{-} \right] \mathrm{d}r \\
&\quad + \frac{1}{\prod_{tt=1}^{N}\Gamma(m_{tt})} \int_0^{Rt} \operatorname{erfc}(\sqrt{br}) F_{\gamma_{\mathrm{SD}}}(r) \frac{1}{r} G_{0,N}^{N,0} \\
&\quad \times \left[\frac{r}{\overline{\gamma}_{\mathrm{RD}}} \prod_{tt=1}^{N} \frac{m_{tt}}{\Omega_{tt}} \Big|_{m_1,\ldots,m_N}^{-} \right] \mathrm{d}r \\
&\quad - \frac{1}{\prod_{t=1}^{N}\Gamma(m_t) \prod_{tt=1}^{N}\Gamma(m_{tt})} \int_0^{Rt} \operatorname{erfc}(\sqrt{br}) F_{\gamma_{\mathrm{SD}}}(r) \frac{1}{r} G_{0,N}^{N,0} \\
&\quad \times \left[\frac{r}{\overline{\gamma}_{\mathrm{SR}}} \prod_{t=1}^{N} \frac{m_t}{\Omega_t} \Big|_{m_1,\ldots,m_N}^{-} \right] G_{1,N+1}^{N,1} \left[\frac{r}{\overline{\gamma}_{\mathrm{RD}}} \prod_{tt=1}^{N} \frac{m_{tt}}{\Omega_{tt}} \Big|_{m_1,\ldots,m_N,0}^{1} \right] \mathrm{d}r \\
&\quad - \frac{1}{\prod_{t=1}^{N}\Gamma(m_t) \prod_{tt=1}^{N}\Gamma(m_{tt})} \int_0^{Rt} \operatorname{erfc}(\sqrt{br}) F_{\gamma_{\mathrm{SD}}}(r) \frac{1}{r} G_{1,N+1}^{N,1} \\
&\quad \times \left[\frac{r}{\overline{\gamma}_{\mathrm{SR}}} \prod_{t=1}^{N} \frac{m_t}{\Omega_t} \Big|_{m_1,\ldots,m_N,0}^{1} \right] G_{0,N}^{N,0} \left[\frac{r}{\overline{\gamma}_{\mathrm{RD}}} \prod_{tt=1}^{N} \frac{m_{tt}}{\Omega_{tt}} \Big|_{m_1,\ldots,m_N}^{-} \right] \mathrm{d}r \\
&= \mathrm{VB}_1 + \mathrm{VB}_2 - \mathrm{VB}_3 - \mathrm{VB}_4.
\end{aligned} \tag{44}
$$

$$
\begin{aligned}
V_5 &= \int_0^{\infty} \operatorname{erfc}(\sqrt{br}) f_{\gamma_{\mathrm{up}}}(r)\mathrm{d}r - \int_0^{Rt} \operatorname{erfc}(\sqrt{br}) f_{\gamma_{\mathrm{up}}}(r)\mathrm{d}r \\
&= \mathrm{VC}_1 - \mathrm{VC}_2.
\end{aligned} \tag{45}
$$

In (43)–(45), Meijer's G-function gives

$$
\begin{aligned}
&G_{1,N+1}^{N,1}\left[\frac{r}{\overline{\gamma}_{\mathrm{SR}}} \prod_{t=1}^{N} \frac{m_t}{\Omega_t} \Big|_{m_1,\ldots,m_N,0}^{1} \right] \\
&= \sum_{h=1}^{N} \frac{\prod_{j=1}^{N}\Gamma(m_j - m_h)\Gamma(m_h)}{\Gamma(1+m_h)} \left(\frac{r}{\overline{\gamma}_{\mathrm{SR}}} \prod_{t=1}^{N} \frac{m_t}{\Omega_t} \right)^{m_h} \\
&\quad \times {}_1F_N\left(m_h; 1+m_h-m_1, \ldots, 1+m_h; (-1)^{-N} \frac{r}{\overline{\gamma}_{\mathrm{SR}}} \prod_{t=1}^{N} \frac{m_t}{\Omega_t} \right) \\
&= \sum_{h=1}^{N} C \sum_{k=0}^{\infty} D (r)^{k+m_h}.
\end{aligned} \tag{46}
$$

$$
\begin{aligned}
C &= \frac{\prod_{j=1}^{N}\Gamma(m_j - m_h)\Gamma(m_h)}{\Gamma(1+m_h)}, \\
D &= \frac{(-1)^{-Nk} \left(\frac{1}{\overline{\gamma}_{\mathrm{SR}}} \prod_{t=1}^{N} \frac{m_t}{\Omega_t} \right)^{k+m_h} (m_h)_k}{(1+m_h-m_1)_k (1+m_h-m_2)_k \cdots (1+m_h)_k k!},
\end{aligned} \tag{47}
$$

and for V_3, V_4, and V_5

$$
\begin{aligned}
\mathrm{VA}_1 &= \frac{1}{\prod_{t=1}^{N}\Gamma(m_t)\prod_{i=1}^{N}\Gamma(m_i)} \times \int_0^{Rt} \frac{1}{\sqrt{\pi}} G_{1,2}^{2,0}\left[br \Big|_{0,\frac{1}{2}}^{1} \right] \frac{1}{r} G_{0,N}^{N,0} \\
&\quad \times \left[\frac{r}{\overline{\gamma}_{SD}} \prod_{i=1}^{N} \frac{m_i}{\Omega_i} \Big|_{m_1,\ldots,m_N}^{-} \right] G_{1,N+1}^{N,1} \left[\frac{r}{\overline{\gamma}_{SR}} \prod_{t=1}^{N} \frac{m_t}{\Omega_t} \Big|_{m_1,\ldots,m_N,0}^{1} \right] \mathrm{d}r \\
&= \frac{1}{\prod_{t=1}^{N}\Gamma(m_t)\prod_{i=1}^{N}\Gamma(m_i)} \int_0^{Rt} \frac{1}{r} G_{0,N}^{N,0} \left[\frac{r}{\overline{\gamma}_{SD}} \prod_{i=1}^{N} \frac{m_i}{\Omega_i} \Big|_{m_1,\ldots,m_N}^{-} \right] G_{1,N+1}^{N,1} \\
&\quad \times \left[\frac{r}{\overline{\gamma}_{SR}} \prod_{t=1}^{N} \frac{m_t}{\Omega_t} \Big|_{m_1,\ldots,m_N,0}^{1} \right] \mathrm{d}r \\
&\quad + \frac{A}{\prod_{t=1}^{N}\Gamma(m_t)\prod_{i=1}^{N}\Gamma(m_i)} \sum_{k=0}^{\infty} B \int_0^{Rt} r^{k-\frac{1}{2}} G_{0,N}^{N,0} \\
&\quad \times \left[\frac{r}{\overline{\gamma}_{SD}} \prod_{i=1}^{N} \frac{m_i}{\Omega_i} \Big|_{m_1,\ldots,m_N}^{-} \right] G_{1,N+1}^{N,1} \left[\frac{r}{\overline{\gamma}_{SR}} \prod_{t=1}^{N} \frac{m_t}{\Omega_t} \Big|_{m_1,\ldots,m_N,0}^{1} \right] \mathrm{d}r \\
&= \frac{1}{\prod_{t=1}^{N}\Gamma(m_t)\prod_{i=1}^{N}\Gamma(m_i)} \sum_{h=1}^{N} C \sum_{k=0}^{\infty} D \int_0^{Rt} r^{k+m_h-1} G_{0,N}^{N,0} \\
&\quad \times \left[\frac{r}{\overline{\gamma}_{SD}} \prod_{i=1}^{N} \frac{m_i}{\Omega_i} \Big|_{m_1,\ldots,m_N}^{-} \right] \mathrm{d}r \\
&\quad + \frac{A}{\prod_{t=1}^{N}\Gamma(m_t)\prod_{i=1}^{N}\Gamma(m_i)} \sum_{k=0}^{\infty} B \sum_{h=1}^{N} C \sum_{k=0}^{\infty} D \int_0^{Rt} r^{2k+m_h-\frac{1}{2}} G_{0,N}^{N,0} \\
&\quad \times \left[\frac{r}{\overline{\gamma}_{SD}} \prod_{i=1}^{N} \frac{m_i}{\Omega_i} \Big|_{m_1,\ldots,m_N}^{-} \right] \mathrm{d}r \\
&= \frac{1}{\prod_{t=1}^{N}\Gamma(m_t)\prod_{i=1}^{N}\Gamma(m_i)} \sum_{h=1}^{N} C \sum_{k=0}^{\infty} D (Rt)^{k+m_h} G_{1,N+1}^{N,1} \\
&\quad \times \left[\frac{R_t}{\overline{\gamma}_{SD}} \prod_{i=1}^{N} \frac{m_i}{\Omega_i} \Big|_{m_1,,m_N,-k-\frac{1}{2}}^{1-k-m_h} \right] \\
&\quad + \frac{A}{\prod_{t=1}^{N}\Gamma(m_t)\prod_{i=1}^{N}\Gamma(m_i)} \sum_{k=0}^{\infty} B \sum_{h=1}^{N} C \sum_{k=0}^{\infty} D (Rt)^{2k+m_h+\frac{1}{2}} G_{1,N+1}^{N,1} \\
&\quad \times \left[\frac{R_t}{\overline{\gamma}_{SD}} \prod_{i=1}^{N} \frac{m_i}{\Omega_i} \Big|_{m_1,\ldots,m_N,-2k-m_h-\frac{1}{2}}^{\frac{1}{2}-2k-m_h} \right].
\end{aligned} \tag{48}
$$

$$
\begin{aligned}
\mathrm{VA}_2 &= \frac{1}{\prod_{t=1}^{N}\Gamma(m_t)} \int_0^{Rt} \operatorname{erfc}(\sqrt{br}) f_{\gamma_{\mathrm{SD}}}(r) G_{1,N+1}^{N,1} \\
&\quad \times \left[\frac{r}{\overline{\gamma}_{\mathrm{RD}}} \prod_{t=1}^{N} \frac{m_t}{\Omega_t} \Big|_{m_1,\ldots,m_N,0}^{1} \right] \mathrm{d}r \\
&= \frac{1}{\prod_{t=1}^{N}\Gamma(m_t)\prod_{i=1}^{N}\Gamma(m_i)} \sum_{h=1}^{N} C \sum_{k=0}^{\infty} E (\mathrm{Rt})^{k+m_h} G_{1,N+1}^{N,1} \\
&\quad \times \left[\frac{R_{\mathrm{t}}}{\overline{\gamma}_{\mathrm{SD}}} \prod_{i=1}^{N} \frac{m_i}{\Omega_i} \Big|_{m_1,\ldots,m_N,-k-\frac{1}{2}}^{1-k-m_h} \right] \\
&\quad + \frac{A}{\prod_{t=1}^{N}\Gamma(m_t)\prod_{i=1}^{N}\Gamma(m_i)} \sum_{k=0}^{\infty} B \sum_{h=1}^{N} C \sum_{k=0}^{\infty} E (\mathrm{Rt})^{2k+m_h+\frac{1}{2}} G_{1,N+1}^{N,1} \\
&\quad \times \left[\frac{R_{\mathrm{t}}}{\overline{\gamma}_{\mathrm{SD}}} \prod_{i=1}^{N} \frac{m_i}{\Omega_i} \Big|_{m_1,\ldots,m_N,-2k-m_h-\frac{1}{2}}^{\frac{1}{2}-2k-m_h} \right].
\end{aligned} \tag{49}
$$

$$E=\frac{(-1)^{-Nk}\left(\frac{1}{\overline{\overline{\gamma_{\mathrm{RD}}}}}\prod_{tt=1}^{N}\frac{m_{tt}}{\Omega_{tt}}\right)^{k+m_h}(m_h)_k}{(1+m_h-m_1)_k(1+m_h-m_2)_k\cdots(1+m_h)_k k!}. \tag{50}$$

$$\begin{aligned}
\mathrm{VA}_3 &= \frac{1}{\prod_{t=1}^{N}\Gamma(m_t)\prod_{tt=1}^{N}\Gamma(m_{tt})\prod_{i=1}^{N}\Gamma(m_i)}\int_0^{R\mathrm{t}}\frac{1}{r}G_{0,N}^{N,0}\\
&\quad\times\left[\frac{r}{\overline{\overline{\gamma_{\mathrm{SD}}}}}\prod_{i=1}^{N}\frac{m_i}{\Omega_i}\Big|_{m_1,\ldots,m_N}^{-}\right]G_{1,N+1}^{N,1}\left[\frac{r}{\overline{\overline{\gamma_{\mathrm{SR}}}}}\prod_{t=1}^{N}\frac{m_t}{\Omega_t}\Big|_{m_1,\ldots,m_N,0}^{1}\right]\\
&\quad\times G_{1,N+1}^{N,1}\left[\frac{r}{\overline{\overline{\gamma_{\mathrm{RD}}}}}\prod_{tt=1}^{N}\frac{m_{tt}}{\Omega_{tt}}\Big|_{m_1,\ldots,m_N,0}^{1}\right]\mathrm{d}r\\
&\quad+\frac{A}{\prod_{t=1}^{N}\Gamma(m_t)\prod_{tt=1}^{N}\Gamma(m_{tt})\prod_{i=1}^{N}\Gamma(m_i)}\sum_{k=0}^{\infty}B\\
&\quad\times\int_0^{R\mathrm{t}}r^{k-\frac{1}{2}}G_{0,N}^{N,0}\left[\frac{r}{\overline{\overline{\gamma_{\mathrm{SD}}}}}\prod_{i=1}^{N}\frac{m_i}{\Omega_i}\Big|_{m_1,\ldots,m_N}^{-}\right]G_{1,N+1}^{N,1}\\
&\quad\times\left[\frac{r}{\overline{\overline{\gamma_{\mathrm{SR}}}}}\prod_{t=1}^{N}\frac{m_t}{\Omega_t}\Big|_{m_1,\ldots,m_N,0}^{1}\right]G_{1,N+1}^{N,1}\left[\frac{r}{\overline{\overline{\gamma_{\mathrm{RD}}}}}\prod_{tt=1}^{N}\frac{m_{tt}}{\Omega_{tt}}\Big|_{m_1,\ldots,m_N,0}^{1}\right]\mathrm{d}r\\
&=\frac{1}{\prod_{t=1}^{N}\Gamma(m_t)\prod_{tt=1}^{N}\Gamma(m_{tt})\prod_{i=1}^{N}\Gamma(m_i)}\\
&\quad\times\sum_{h=1}^{N}C\sum_{k=0}^{\infty}D\int_0^{R\mathrm{t}}r^{k+m_h-1}G_{0,N}^{N,0}\left[\frac{r}{\overline{\overline{\gamma_{\mathrm{SD}}}}}\prod_{i=1}^{N}\frac{m_i}{\Omega_i}\Big|_{m_1,\ldots,m_N}^{-}\right]G_{1,N+1}^{N,1}\\
&\quad\times\left[\frac{r}{\overline{\overline{\gamma_{\mathrm{RD}}}}}\prod_{tt=1}^{N}\frac{m_{tt}}{\Omega_{tt}}\Big|_{m_1,\ldots,m_N,0}^{1}\right]\mathrm{d}r\\
&\quad+\frac{A}{\prod_{t=1}^{N}\Gamma(m_t)\prod_{tt=1}^{N}\Gamma(m_{tt})\prod_{i=1}^{N}\Gamma(m_i)}\\
&\quad\times\sum_{k=0}^{\infty}B\sum_{h=1}^{N}C\sum_{k=0}^{\infty}D\int_0^{R\mathrm{t}}r^{2k+m_h-\frac{1}{2}}G_{0,N}^{N,0}\\
&\quad\times\left[\frac{r}{\overline{\overline{\gamma_{\mathrm{SD}}}}}\prod_{i=1}^{N}\frac{m_i}{\Omega_i}\Big|_{m_1,\ldots,m_N}^{-}\right]G_{1,N+1}^{N,1}\left[\frac{r}{\overline{\overline{\gamma_{\mathrm{RD}}}}}\prod_{tt=1}^{N}\frac{m_{tt}}{\Omega_{tt}}\Big|_{m_1,\ldots,m_N,0}^{1}\right]\mathrm{d}r\\
&=\frac{1}{\prod_{t=1}^{N}\Gamma(m_t)\prod_{tt=1}^{N}\Gamma(m_{tt})\prod_{i=1}^{N}\Gamma(m_i)}\\
&\quad\times\sum_{h=1}^{N}C\sum_{k=0}^{\infty}D\sum_{h=1}^{N}C\sum_{k=0}^{\infty}EG_{1,N+1}^{N,1}\\
&\quad\times\left[\frac{R_{\mathrm{t}}}{\overline{\overline{\gamma_{\mathrm{SD}}}}}\prod_{i=1}^{N}\frac{m_i}{\Omega_i}\Big|_{m_1,\ldots,m_N,-2k-2m_h-\frac{1}{2}}^{\frac{1}{2}-2k-2m_h}\right]\\
&\quad+\frac{A}{\prod_{t=1}^{N}\Gamma(m_t)\prod_{tt=1}^{N}\Gamma(m_{tt})\prod_{i=1}^{N}\Gamma(m_i)}\\
&\quad\times\sum_{k=0}^{\infty}B\sum_{h=1}^{N}C\sum_{k=0}^{\infty}D\sum_{h=1}^{N}C\sum_{k=0}^{\infty}E(R\mathrm{t})^{3k+2m_h+\frac{1}{2}}G_{1,N+1}^{N,1}\\
&\quad\times\left[\frac{R_{\mathrm{t}}}{\overline{\overline{\gamma_{\mathrm{SD}}}}}\prod_{i=1}^{N}\frac{m_i}{\Omega_i}\Big|_{m_1,\ldots,m_N,-3k-2m_h-\frac{1}{2}}^{\frac{1}{2}-3k-2m_h}\right].
\end{aligned} \tag{51}$$

$$\begin{aligned}
\mathrm{VB}_1 &= \frac{1}{\prod_{t=1}^{N}\Gamma(m_t)}\int_0^{R\mathrm{t}}\mathrm{erfc}(\sqrt{br})F_{\gamma_{\mathrm{SD}}}(r)\frac{1}{r}G_{0,N}^{N,0}\\
&\quad\times\left[\frac{r}{\overline{\overline{\gamma_{\mathrm{SR}}}}}\prod_{t=1}^{N}\frac{m_t}{\Omega_t}\Big|_{m_1,\ldots,m_N}^{-}\right]\mathrm{d}r\\
&=\frac{1}{\prod_{t=1}^{N}\Gamma(m_t)\prod_{i=1}^{N}\Gamma(m_i)}\sum_{h=1}^{N}C\sum_{k=0}^{\infty}F(R\mathrm{t})^{k+m_h}G_{1,N+1}^{N,1}\\
&\quad\times\left[\frac{R_{\mathrm{t}}}{\overline{\overline{\gamma_{\mathrm{SR}}}}}\prod_{t=1}^{N}\frac{m_t}{\Omega_t}\Big|_{m_1,\ldots,m_N,-k-\frac{1}{2}}^{1-k-m_h}\right]\\
&\quad+\frac{A}{\prod_{t=1}^{N}\Gamma(m_t)\prod_{i=1}^{N}\Gamma(m_i)}\\
&\quad\times\sum_{k=0}^{\infty}B\sum_{h=1}^{N}C\sum_{k=0}^{\infty}F(R\mathrm{t})^{2k+m_h+\frac{1}{2}}G_{1,N+1}^{N,1}\\
&\quad\times\left[\frac{R_{\mathrm{t}}}{\overline{\overline{\gamma_{\mathrm{SR}}}}}\prod_{t=1}^{N}\frac{m_t}{\Omega_t}\Big|_{m_1,\ldots,m_N,-2k-m_h-\frac{1}{2}}^{\frac{1}{2}-2k-m_h}\right].
\end{aligned} \tag{52}$$

$$F=\frac{(-1)^{-Nk}\left(\frac{1}{\overline{\overline{\gamma_{\mathrm{SD}}}}}\prod_{i=1}^{N}\frac{m_i}{\Omega_i}\right)^{k+m_h}(m_h)_k}{(1+m_h-m_1)_k(1+m_h-m_2)_k\cdots(1+m_h)_k k!}. \tag{53}$$

$$\begin{aligned}
\mathrm{VB}_2 &= \frac{1}{\prod_{tt=1}^{N}\Gamma(m_{tt})}\int_0^{R\mathrm{t}}\mathrm{erfc}(\sqrt{br})F_{\gamma_{\mathrm{SD}}}(r)\frac{1}{r}G_{0,N}^{N,0}\\
&\quad\times\left[\frac{r}{\overline{\overline{\gamma_{\mathrm{RD}}}}}\prod_{tt=1}^{N}\frac{m_{tt}}{\Omega_{tt}}\Big|_{m_1,\ldots,m_N}^{-}\right]\mathrm{d}r\\
&=\frac{1}{\prod_{tt=1}^{N}\Gamma(m_{tt})\prod_{i=1}^{N}\Gamma(m_i)}\sum_{h=1}^{N}C\sum_{k=0}^{\infty}F(R\mathrm{t})^{k+m_h}G_{1,N+1}^{N,1}\\
&\quad\times\left[\frac{R_{\mathrm{t}}}{\overline{\overline{\gamma_{\mathrm{RD}}}}}\prod_{tt=1}^{N}\frac{m_{tt}}{\Omega_{tt}}\Big|_{m_1,\ldots,m_N,-k-\frac{1}{2}}^{1-k-m_h}\right]\\
&\quad+\frac{A}{\prod_{tt=1}^{N}\Gamma(m_{tt})\prod_{i=1}^{N}\Gamma(m_i)}\sum_{k=0}^{\infty}B\\
&\quad\times\sum_{h=1}^{N}C\sum_{k=0}^{\infty}F(R\mathrm{t})^{2k+m_h+\frac{1}{2}}G_{1,N+1}^{N,1}\\
&\quad\times\left[\frac{R_{\mathrm{t}}}{\overline{\overline{\gamma_{\mathrm{RD}}}}}\prod_{tt=1}^{N}\frac{m_{tt}}{\Omega_{tt}}\Big|_{m_1,\ldots,m_N,-2k-m_h-\frac{1}{2}}^{\frac{1}{2}-2k-m_h}\right].
\end{aligned} \tag{54}$$

$$
\begin{aligned}
\mathrm{VB}_3 &= \frac{1}{\prod_{t=1}^{N}\Gamma(m_t)\prod_{tt=1}^{N}\Gamma(m_{tt})\prod_{i=1}^{N}\Gamma(m_i)} \\
&\quad\times\int_0^{R\mathrm{t}}\mathrm{erfc}(\sqrt{br})F_{\gamma_{\mathrm{SD}}}(r)\frac{1}{r}G_{0,N}^{N,0}\left[\frac{r}{\overline{\gamma}_{\mathrm{SR}}}\prod_{t=1}^{N}\frac{m_t}{\Omega_t}\Big|_{m_1,\ldots,m_N}^{-}\right]G_{1,N+1}^{N,1} \\
&\quad\times\left[\frac{r}{\overline{\gamma}_{\mathrm{RD}}}\prod_{tt=1}^{N}\frac{m_{tt}}{\Omega_{tt}}\Big|_{m_1,\ldots,m_N,0}^{1}\right]\mathrm{d}r \\
&= \frac{1}{\prod_{t=1}^{N}\Gamma(m_t)\prod_{tt=1}^{N}\Gamma(m_{tt})\prod_{i=1}^{N}\Gamma(m_i)} \\
&\quad\times\sum_{h=1}^{N}C\sum_{k=0}^{\infty}F\sum_{h=1}^{N}C\sum_{k=0}^{\infty}E(R\mathrm{t})^{2k+2m_h+\frac{1}{2}}G_{1,N+1}^{N,1} \\
&\quad\times\left[\frac{R_{\mathrm{t}}}{\overline{\gamma}_{\mathrm{SR}}}\prod_{t=1}^{N}\frac{m_t}{\Omega_t}\Big|_{m_1,\ldots,m_N,-2k-2m_h-\frac{1}{2}}^{\frac{1}{2}-2k-2m_h}\right] \\
&\quad+\frac{A}{\prod_{t=1}^{N}\Gamma(m_t)\prod_{tt=1}^{N}\Gamma(m_{tt})\prod_{i=1}^{N}\Gamma(m_i)} \\
&\quad\times\sum_{k=0}^{\infty}B\sum_{h=1}^{N}C\sum_{k=0}^{\infty}F\sum_{h=1}^{N}C\sum_{k=0}^{\infty}E(R\mathrm{t})^{3k+2m_h+\frac{1}{2}}G_{1,N+1}^{N,1} \\
&\quad\times\left[\frac{R_{\mathrm{t}}}{\overline{\gamma}_{\mathrm{SR}}}\prod_{t=1}^{N}\frac{m_t}{\Omega_t}\Big|_{m_1,\ldots,m_N,-3k-2m_h-\frac{1}{2}}^{\frac{1}{2}-3k-2m_h}\right].
\end{aligned}
\tag{55}
$$

$$
\begin{aligned}
\mathrm{VB}_4 &= \frac{1}{\prod_{t=1}^{N}\Gamma(m_t)\prod_{tt=1}^{N}\Gamma(m_{tt})}\int_0^{R\mathrm{t}}\mathrm{erfc}(\sqrt{br})F_{\gamma_{\mathrm{SD}}}(r)G_{1,N+1}^{N,1} \\
&\quad\times\left[\frac{r}{\overline{\gamma}_{\mathrm{SR}}}\prod_{t=1}^{N}\frac{m_t}{\Omega_t}\Big|_{m_1,\ldots,m_N,0}^{1}\right]\frac{1}{r}G_{0,N}^{N,0}\left[\frac{r}{\overline{\gamma}_{\mathrm{RD}}}\prod_{tt=1}^{N}\frac{m_{tt}}{\Omega_{tt}}\Big|_{m_1,\ldots,m_N}^{-}\right]\mathrm{d}r \\
&= \frac{1}{\prod_{t=1}^{N}\Gamma(m_t)\prod_{tt=1}^{N}\Gamma(m_{tt})\prod_{i=1}^{N}\Gamma(m_i)} \\
&\quad\times\sum_{h=1}^{N}C\sum_{k=0}^{\infty}F\sum_{h=1}^{N}C\sum_{k=0}^{\infty}D(R\mathrm{t})^{2k+2m_h+\frac{1}{2}}G_{1,N+1}^{N,1} \\
&\quad\times\left[\frac{R_{\mathrm{t}}}{\overline{\gamma}_{\mathrm{RD}}}\prod_{tt=1}^{N}\frac{m_{tt}}{\Omega_{tt}}\Big|_{m_1,\ldots,m_N,-2k-2m_h-\frac{1}{2}}^{\frac{1}{2}-2k-2m_h}\right] \\
&\quad+\frac{A}{\prod_{t=1}^{N}\Gamma(m_t)\prod_{tt=1}^{N}\Gamma(m_{tt})\prod_{i=1}^{N}\Gamma(m_i)} \\
&\quad\times\sum_{k=0}^{\infty}B\sum_{h=1}^{N}C\sum_{k=0}^{\infty}F\sum_{h=1}^{N}C\sum_{k=0}^{\infty}D(R\mathrm{t})^{3k+2m_h+\frac{1}{2}}G_{1,N+1}^{N,1} \\
&\quad\times\left[\frac{R_{\mathrm{t}}}{\overline{\gamma}_{\mathrm{RD}}}\prod_{tt=1}^{N}\frac{m_{tt}}{\Omega_{tt}}\Big|_{m_1,\ldots,m_N,-3k-2m_h-\frac{1}{2}}^{\frac{1}{2}-3k-2m_h}\right].
\end{aligned}
\tag{56}
$$

$$
\begin{aligned}
\mathrm{VC}_1 &= \int_0^{\infty}\mathrm{erfc}(\sqrt{br})f_{\gamma_{\mathrm{up}}}(r)\mathrm{d}r \\
&= \frac{1}{\sqrt{\pi}\prod_{t=1}^{N}\Gamma(m_t)}G_{2,N+1}^{N,2}\left[\frac{1}{b\overline{\gamma}_{\mathrm{SR}}}\prod_{t=1}^{N}\frac{m_t}{\Omega_t}\Big|_{m_1,\ldots,m_N,0}^{1,\frac{1}{2}}\right] \\
&\quad+\frac{1}{\sqrt{\pi}\prod_{tt=1}^{N}\Gamma(m_{tt})}G_{2,N+1}^{N,2}\left[\frac{1}{b\overline{\gamma}_{\mathrm{RD}}}\prod_{tt=1}^{N}\frac{m_{tt}}{\Omega_{tt}}\Big|_{m_1,\ldots,m_N,0}^{1,\frac{1}{2}}\right]-\mathrm{VD}.
\end{aligned}
\tag{57}
$$

$$
\begin{aligned}
\mathrm{VC}_2 &= \int_0^{R\mathrm{t}}\mathrm{erfc}\left(\sqrt{br}\right)f_{\gamma_{\mathrm{up}}}(r)\mathrm{d}r \\
&= \frac{1}{\prod_{t=1}^{N}\Gamma(m_t)}\int_0^{R\mathrm{t}}\mathrm{erfc}\left(\sqrt{br}\right)\frac{1}{r}G_{0,N}^{N,0}\left[\frac{r}{\overline{\gamma}_{\mathrm{SR}}}\prod_{t=1}^{N}\frac{m_t}{\Omega_t}\Big|_{m_1,\ldots,m_N}^{-}\right]\mathrm{d}r \\
&\quad+\frac{1}{\prod_{tt=1}^{N}\Gamma(m_{tt})}\int_0^{R\mathrm{t}}\mathrm{erfc}\left(\sqrt{br}\right)\frac{1}{r}G_{0,N}^{N,0}\left[\frac{r}{\overline{\gamma}_{\mathrm{RD}}}\prod_{tt=1}^{N}\frac{m_{tt}}{\Omega_{tt}}\Big|_{m_1,\ldots,m_N}^{-}\right]\mathrm{d}r \\
&\quad-\frac{1}{\prod_{t=1}^{N}\Gamma(m_t)\prod_{tt=1}^{N}\Gamma(m_{tt})}\int_0^{R\mathrm{t}}\mathrm{erfc}\left(\sqrt{br}\right)\frac{1}{r}G_{0,N}^{N,0} \\
&\quad\times\left[\frac{r}{\overline{\gamma}_{\mathrm{SR}}}\prod_{t=1}^{N}\frac{m_t}{\Omega_t}\Big|_{m_1,\ldots,m_N}^{-}\right]G_{1,N+1}^{N,1}\left[\frac{r}{\overline{\gamma}_{\mathrm{RD}}}\prod_{tt=1}^{N}\frac{m_{tt}}{\Omega_{tt}}\Big|_{m_1,\ldots,m_N,0}^{1}\right]\mathrm{d}r \\
&\quad-\frac{1}{\prod_{t=1}^{N}\Gamma(m_t)\prod_{tt=1}^{N}\Gamma(m_{tt})}\int_0^{R\mathrm{t}}\mathrm{erfc}\left(\sqrt{br}\right)G_{1,N+1}^{N,1} \\
&\quad\times\left[\frac{r}{\overline{\gamma}_{\mathrm{SR}}}\prod_{t=1}^{N}\frac{m_t}{\Omega_t}\Big|_{m_1,\ldots,m_N,0}^{1}\right]\frac{1}{r}G_{0,N}^{N,0}\left[\frac{r}{\overline{\gamma}_{\mathrm{RD}}}\prod_{tt=1}^{N}\frac{m_{tt}}{\Omega_{tt}}\Big|_{m_1,\ldots,m_N}^{-}\right]\mathrm{d}r \\
&= \mathrm{VE}_1+\mathrm{VE}_2-\mathrm{VE}_3-\mathrm{VE}_4.
\end{aligned}
\tag{58}
$$

$$
\begin{aligned}
\mathrm{VE}_1 &= \frac{1}{\prod_{t=1}^{N}\Gamma(m_t)}\int_0^{R\mathrm{t}}\mathrm{erfc}(\sqrt{br})\frac{1}{r}G_{0,N}^{N,0}\left[\frac{r}{\overline{\gamma}_{\mathrm{SR}}}\prod_{t=1}^{N}\frac{m_t}{\Omega_t}\Big|_{m_1,\ldots,m_N}^{-}\right]\mathrm{d}r \\
&= \frac{1}{\prod_{t=1}^{N}\Gamma(m_t)}G_{1,N+1}^{N,1}\left[\frac{R_{\mathrm{t}}}{\overline{\gamma}_{\mathrm{SR}}}\prod_{t=1}^{N}\frac{m_t}{\Omega_t}\Big|_{m_1,\ldots,m_N,0}^{1}\right] \\
&\quad+\frac{A}{\prod_{t=1}^{N}\Gamma(m_t)}\sum_{k=0}^{\infty}BG_{1,N+1}^{N,1}\left[\frac{R_{\mathrm{t}}}{\overline{\gamma}_{\mathrm{SR}}}\prod_{t=1}^{N}\frac{m_t}{\Omega_t}\Big|_{m_1,\ldots,m_N,0}^{1}\right].
\end{aligned}
\tag{59}
$$

$$
\begin{aligned}
\mathrm{VE}_2 &= \frac{1}{\prod_{tt=1}^{N}\Gamma(m_{tt})}\int_0^{R\mathrm{t}}\mathrm{erfc}\left(\sqrt{br}\right)\frac{1}{r}G_{0,N}^{N,0}\left[\frac{r}{\overline{\gamma}_{\mathrm{RD}}}\prod_{tt=1}^{N}\frac{m_{tt}}{\Omega_{tt}}\Big|_{m_1,\ldots,m_N}^{-}\right]\mathrm{d}r \\
&= \frac{1}{\prod_{tt=1}^{N}\Gamma(m_{tt})}G_{1,N+1}^{N,1}\left[\frac{R_{\mathrm{t}}}{\overline{\gamma}_{\mathrm{RD}}}\prod_{tt=1}^{N}\frac{m_{tt}}{\Omega_{tt}}\Big|_{m_1,\ldots,m_N,0}^{1}\right] \\
&\quad+\frac{A}{\prod_{t=1}^{N}\Gamma(m_t)}\sum_{k=0}^{\infty}BG_{1,N+1}^{N,1}\left[\frac{R_{\mathrm{t}}}{\overline{\gamma}_{\mathrm{RD}}}\prod_{tt=1}^{N}\frac{m_{tt}}{\Omega_{tt}}\Big|_{m_1,\ldots,m_N,0}^{1}\right].
\end{aligned}
\tag{60}
$$

$$
\begin{aligned}
\mathrm{VE}_3 &= \frac{1}{\prod_{t=1}^{N}\Gamma(m_t)\prod_{tt=1}^{N}\Gamma(m_{tt})}\int_0^{R\mathrm{t}}\mathrm{erfc}(\sqrt{br})\frac{1}{r}G_{0,N}^{N,0} \\
&\quad\times\left[\frac{r}{\overline{\gamma}_{\mathrm{SR}}}\prod_{t=1}^{N}\frac{m_t}{\Omega_t}\Big|_{m_1,\ldots,m_N}^{-}\right]G_{1,N+1}^{N,1}\left[\frac{r}{\overline{\gamma}_{\mathrm{RD}}}\prod_{tt=1}^{N}\frac{m_{tt}}{\Omega_{tt}}\Big|_{m_1,\ldots,m_N,0}^{1}\right]\mathrm{d}r \\
&= \frac{1}{\prod_{t=1}^{N}\Gamma(m_t)\prod_{tt=1}^{N}\Gamma(m_{tt})}\sum_{h=1}^{N}C\sum_{k=0}^{\infty}E(R\mathrm{t})^{k+m_h}G_{1,N+1}^{N,1} \\
&\quad\times\left[\frac{R_{\mathrm{t}}}{\overline{\gamma}_{\mathrm{SR}}}\prod_{t=1}^{N}\frac{m_t}{\Omega_t}\Big|_{m_1,\ldots,m_N,-k-\frac{1}{2}}^{1-k-m_h}\right] \\
&\quad+\frac{A}{\prod_{t=1}^{N}\Gamma(m_t)\prod_{tt=1}^{N}\Gamma(m_{tt})} \\
&\quad\times\sum_{k=0}^{\infty}B\sum_{h=1}^{N}C\sum_{k=0}^{\infty}E(R\mathrm{t})^{2k+m_h+\frac{1}{2}}G_{1,N+1}^{N,1} \\
&\quad\times\left[\frac{R_{\mathrm{t}}}{\overline{\gamma}_{\mathrm{SR}}}\prod_{t=1}^{N}\frac{m_t}{\Omega_t}\Big|_{m_1,\ldots,m_N,-2k-m_h-\frac{1}{2}}^{\frac{1}{2}-2k-m_h}\right].
\end{aligned}
\tag{61}
$$

$$
\begin{aligned}
\mathrm{VE}_4 &= \frac{1}{\prod_{t=1}^{N}\Gamma(m_t)\prod_{tt=1}^{N}\Gamma(m_{tt})}\int_0^{\mathrm{Rt}}\operatorname{erfc}(\sqrt{br})G_{1,N+1}^{N,1}\\
&\quad\times\left[\frac{r}{\overline{\gamma}_{\mathrm{SR}}}\prod_{t=1}^{N}\frac{m_t}{\Omega_t}\Big|_{m_1,\ldots,m_N,0}^{1}\right]\frac{1}{r}G_{0,N}^{N,0}\left[\frac{r}{\overline{\gamma}_{\mathrm{RD}}}\prod_{tt=1}^{N}\frac{m_{tt}}{\Omega_{tt}}\Big|_{m_1,\ldots,m_N}^{-}\right]\mathrm{d}r\\
&= \frac{1}{\prod_{t=1}^{N}\Gamma(m_t)\prod_{tt=1}^{N}\Gamma(m_{tt})}\sum_{h=1}^{N}C\sum_{k=0}^{\infty}D(\mathrm{Rt})^{k+m_h}G_{1,N+1}^{N,1}\\
&\quad\times\left[\frac{R_{\mathrm{t}}}{\overline{\gamma}_{\mathrm{RD}}}\prod_{tt=1}^{N}\frac{m_{tt}}{\Omega_{tt}}\Big|_{m_1,\ldots,m_N,-k-\frac{1}{2}}^{1-k-m_h}\right]\\
&\quad+\frac{A}{\prod_{t=1}^{N}\Gamma(m_t)\prod_{tt=1}^{N}\Gamma(m_{tt})}\\
&\quad\times\sum_{k=0}^{\infty}B\sum_{h=1}^{N}C\sum_{k=0}^{\infty}D(\mathrm{Rt})^{2k+m_h+\frac{1}{2}}G_{1,N+1}^{N,1}\\
&\quad\times\left[\frac{R_{\mathrm{t}}}{\overline{\gamma}_{\mathrm{RD}}}\prod_{tt=1}^{N}\frac{m_{tt}}{\Omega_{tt}}\Big|_{m_1,\ldots,m_N,-2k-m_h-\frac{1}{2}}^{\frac{1}{2}-2k-m_h}\right].
\end{aligned}
\tag{62}
$$

$$
\begin{aligned}
\mathrm{VD} &= \frac{1}{\sqrt{\pi}\prod_{t=1}^{N}\Gamma(m_t)\prod_{tt=1}^{N}\Gamma(m_{tt})}\int_0^{\infty}\frac{1}{r}G_{1,2}^{2,0}\left(br\Big|_{0,\frac{1}{2}}^{1}\right)\\
&\quad\times\left(\begin{array}{l}G_{0,N}^{N,0}\left[\frac{r}{\overline{\gamma}_{\mathrm{SR}}}\prod_{t=1}^{N}\frac{m_t}{\Omega_t}\Big|_{m_1,\ldots,m_N}^{-}\right]G_{1,N+1}^{N,1}\left[\frac{r}{\overline{\gamma}_{\mathrm{RD}}}\prod_{tt=1}^{N}\frac{m_{tt}}{\Omega_{tt}}\Big|_{m_1,\ldots,m_N,0}^{1}\right]\\ +G_{1,N+1}^{N,1}\left[\frac{r}{\overline{\gamma}_{\mathrm{SR}}}\prod_{t=1}^{N}\frac{m_t}{\Omega_t}\Big|_{m_1,\ldots,m_N,0}^{1}\right]G_{0,N}^{N,0}\left[\frac{r}{\overline{\gamma}_{\mathrm{RD}}}\prod_{tt=1}^{N}\frac{m_{tt}}{\Omega_{tt}}\Big|_{m_1,\ldots,m_N}^{-}\right]\end{array}\right)\mathrm{d}r\\
&= \frac{1}{\sqrt{\pi}\prod_{i=1}^{N}\Gamma(m_i)\prod_{tt=1}^{N}\Gamma(m_{tt})}\\
&\quad\times\left(G_{2,1:0,N:N,1}^{0,2:N,0:N,1}\left[\begin{matrix}1,\frac{1}{2}\\0\end{matrix}\Big|\begin{matrix}-\\m_1,\ldots,m_N\end{matrix}\Big|\begin{matrix}1\\m_1,\ldots,m_N,0\end{matrix}\Big|\begin{matrix}\frac{1}{b\overline{\gamma}_{\mathrm{SR}}}\prod_{t=1}^{N}\frac{m_t}{\Omega_t},\frac{1}{b\overline{\gamma}_{\mathrm{RD}}}\prod_{tt=1}^{N}\frac{m_{tt}}{\Omega_{tt}}\end{matrix}\right]\right.\\
&\quad\left.+G_{2,1:0,N:1,N+1}^{0,2:N,0:N,1}\left[\begin{matrix}1,\frac{1}{2}\\0\end{matrix}\Big|\begin{matrix}-\\m_1,\ldots,m_N\end{matrix}\Big|\begin{matrix}1\\m_1,\ldots,m_N,0\end{matrix}\Big|\begin{matrix}\frac{1}{b\overline{\gamma}_{\mathrm{RD}}}\prod_{tt=1}^{N}\frac{m_{tt}}{\Omega_{tt}},\frac{1}{b\overline{\gamma}_{\mathrm{SR}}}\prod_{t=1}^{N}\frac{m_t}{\Omega_t}\end{matrix}\right]\right).
\end{aligned}
\tag{63}
$$

Equations (24)–(63) are used to obtain the analytical results.

6 ABEP performance prediction based on a BP neural network

6.1 Selection of input and output

The ABEP performance is affected significantly by m, N, V, and K. We therefore use 11 indicators as the input X, and the ABEP performance is output Y. The 11 indicators are m_{SR}, m_{RD}, m_{SD}, G_{SR}, G_{RD}, N_{SR}, N_{RD}, N_{SD}, K, R_{t}, $\bar{\gamma}$ so X is

$$X = (x_1, x_2, \ldots, x_{11}). \tag{64}$$

6.2 BP neural network structure

The BP neural network is shown in Fig. 2. For the input layer, there are 11 neurons, for the hidden layer, there are q neurons and for the output layer, there is 1 neuron. For the input and hidden layers, w_{ij} is the weight coefficient and b_j is the bias value. For the hidden and output layers, v_j is the weight coefficient and θ is the bias value. The network steps are as follows.

(1) For the hidden layer, the input is

$$s_j = \sum_{i=1}^{11} w_{ij}x_i + b_j, \quad j = 1, 2, \ldots, q, \tag{65}$$

and the corresponding output is

$$c_j = f(s_j), \tag{66}$$

where $f(\mathrm{x})$ is the activation function.

For the output layer, the input is

$$\beta = \sum_{j=1}^{q} v_j c_j + \theta. \tag{67}$$

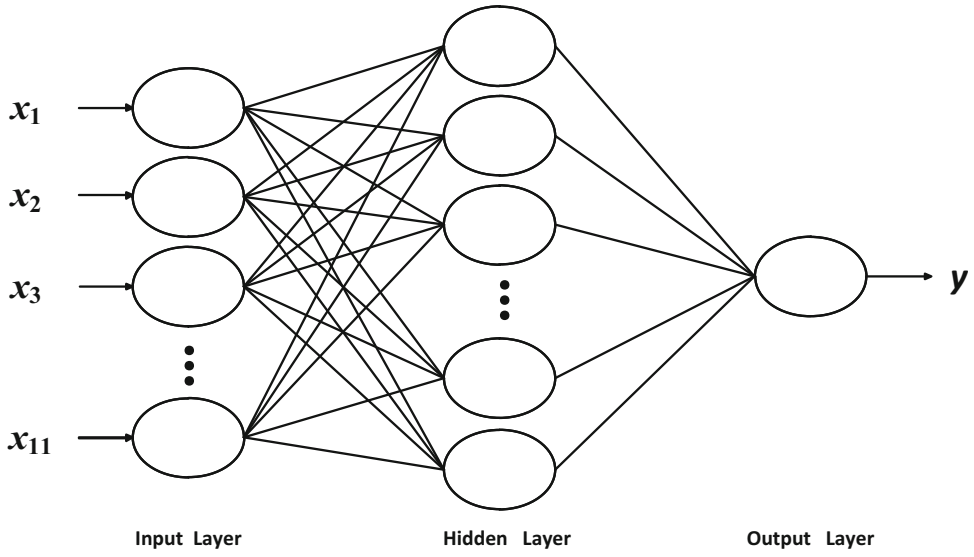

Fig. 2 The BP neural network structure

and the corresponding output is

$$o = f(\beta). \tag{68}$$

P is the number of training data. For tth output neuron, o^l is the output for the lth training data, and the error is given by

$$EE^l = \left(d^l - o^l\right)^2, \tag{69}$$

where d^l is the desired output.The overall output error E of P training data is

$$EE = \sum_{l=1}^{P} \left(d^l - o^l\right)^2. \tag{70}$$

(2) For the different layers, the weights and biases are as follows.

The error of the output layer is

$$\delta = (d - o)(1 - o), \tag{71}$$

and the error of the hidden layer is

$$\sigma_j = \delta v_j (1 - y_j). \tag{72}$$

The weights and thresholds are

$$v_j = v_j + \eta \delta y_j, \tag{73}$$

$$\theta = \theta + \eta \delta, \tag{74}$$

$$w_{ij} = w_{ij} + a\sigma_j x_i, \tag{75}$$

$$b_j = b_j + a\sigma_j, \tag{76}$$

where η is the weight adjustment parameter, $0 < \eta < 1$, and a is the learning coefficient, $0 < a < 1$.

6.3 ABEP performance prediction based on a BP neural network

Figure 3 shows the flowchart of the OP performance prediction algorithm. The algorithm steps are as follows.

(1) Data collection and preparation. We use the derived closed-form expressions to generate 1000 groups of data. 950 groups are used for training, and 50 groups are used for testing. The groups of data are normalized.
(2) Network initialization. To initialize the biases and weights, small random numbers are used. We also set the minimum error, maximum number of iterations, and the learning rate.
(3) Network training. We provide input X and output Y which are randomly selected. During training, the network output of each layer and the training error are calculated, and the biases and weights of the layers are adjusted. When the learning converges or the error is less than the minimum, the training stops.
(4) When model training is completed, the network structure is saved. Then, the testing data are used to detect whether it meets the accuracy requirements.
(5) If the accuracy requirements are met, the network structure is used for ABEP performance prediction and the optimal weights and biases are obtained.

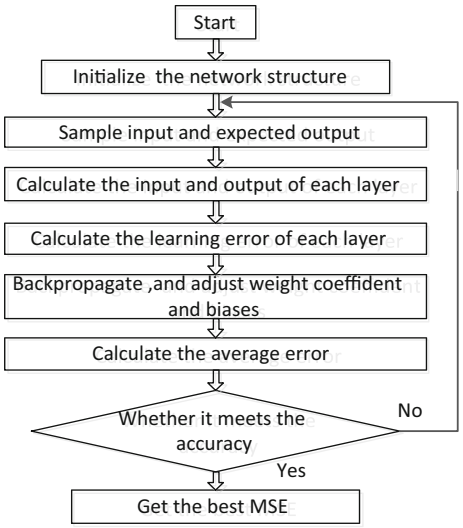

Fig. 3 The flowchart of the OP performance prediction algorithm

6.4 Metric

We use the mean squared error (MSE) to evaluate the performance. A higher prediction accuracy means a smaller MSE. The MSE is given by

$$\text{MSE} = \frac{\sum_{l=1}^{PP} \left(d^l - o^l\right)^2}{PP}, \tag{77}$$

where PP is the number of testing data.

7 Performance results

In this section, QPSK modulation is considered with $E = 1$ and $\mu = G_{SR}/G_{RD}$. Figure 4 presents the ABEP performance comparison with the parameters given in Table 1. The ABEP performance of IAF is the best and the performance of direct communication is the worst. For SNR = 16 dB, the ABEP is 2×10^{-3} with IAF, 1.1×10^{-2} with end-to-end communication, and 2×10^{-2} with direct communication.

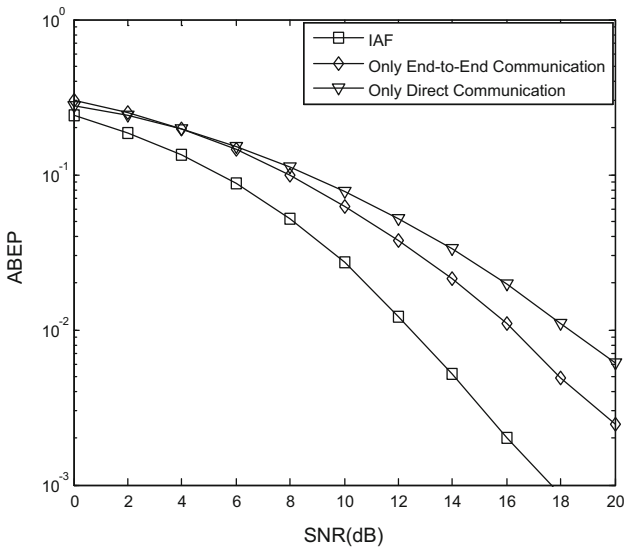

Fig. 4 The ABEP performance comparison

Table 1 The parameters for ABEP performance comparison

μ	0 dB
K	0.5
Rt	8 dB
m_{SD}	2
m_{SR}	2
m_{RD}	2
N_{SD}	2
N_{SR}	2
N_{RD}	2

Figure 5 presents the ABEP performance for $\mu = 0$ dB, $K = 0.5$, and Rt = 4 dB with the combinations of N and m given in Table 2. These results show that the theoretical and simulation results are similar, which verifies the theoretical results. Further, the ABEP improves as the SNR increases.

The effect of Rt on the ABEP performance is presented in Fig. 6 for $\mu = 0$ dB, $K = 0.5$, $N = 2$, $m = 2$, and Rt = -4 dB, 0 dB, and 4 dB. This shows that the ABEP improves as Rt is increased. This is because the probability that the MR cooperates increases with Rt. When SNR = 14 dB, the ABEP is 3×10^{-2} for Rt = -4 dB, 2×10^{-2} for Rt = 0 dB, and 9×10^{-3} for Rt = 4 dB. Further, the ABEP is better than that with direct transmission alone.

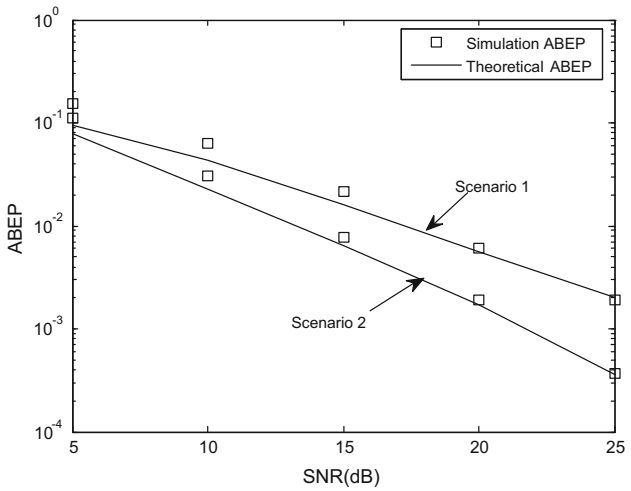

Fig. 5 The ABEP performance for two scenarios

Table 2 The parameters for two scenarios

	Scenario 1	Scenario 2
m_{SD}	1	2
m_{SR}	1	2
m_{RD}	1	2
N_{SD}	2	2
N_{SR}	2	2
N_{RD}	2	2

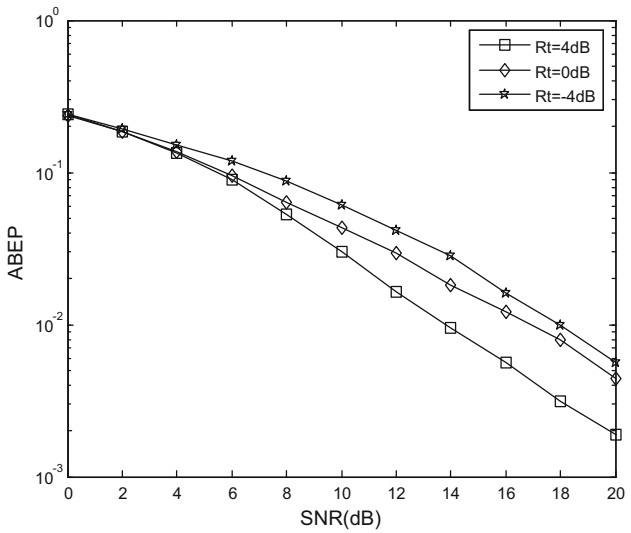

Fig. 6 The effect of Rt on the ABEP performance

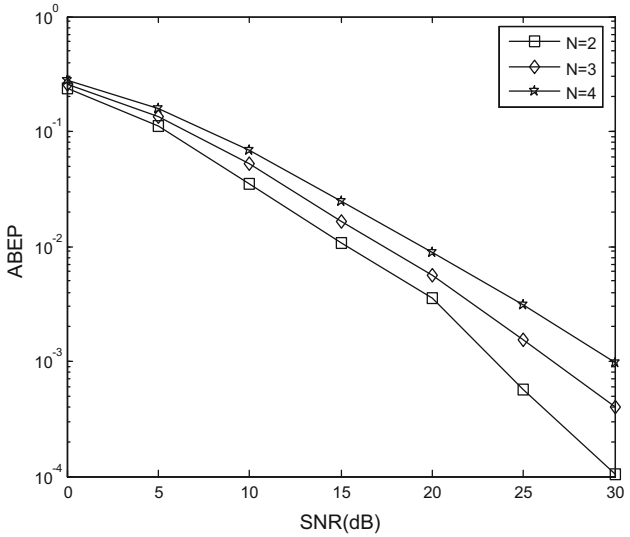

Fig. 7 The effect of N on the ABEP performance

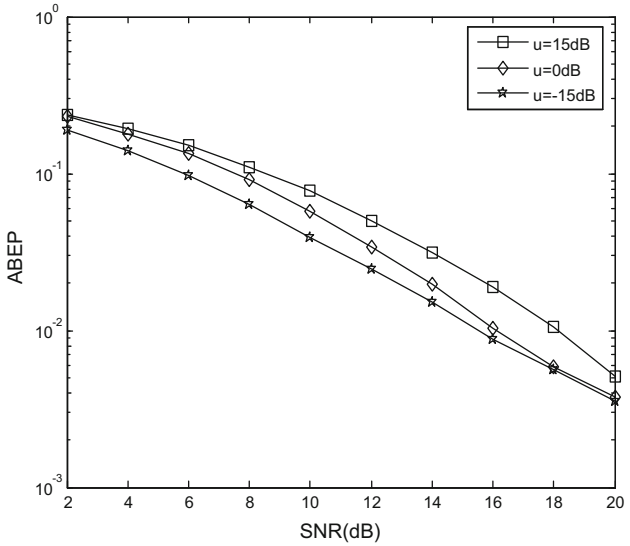

Fig. 8 The effect of μ on the ABEP performance

The effect of N on the ABEP performance is given in Fig. 7 for $N = 2, 3, 4$, $m = 2$, $\mu = 0$ dB, Rt = 2 dB, and $K = 0.5$. Figure 7 shows that the ABEP performance degrades as N increases. This is because a larger N results in more severe N-Nakagami fading channels.

The effect of μ on the ABEP performance is given in Fig. 8 for $\mu = 15$ dB, 0 dB, $-$ 15 dB, Rt = 2 dB, $N = 2$, $K = 0.5$, and $m = 2$. As μ is reduced, this shows that the ABEP is improved. These results indicate that the MR should be located near the MD.

The effect of m on the ABEP performance is given in Fig. 9 for $N = 2$, $m = 1, 2, 3$, $\mu = 0$ dB, Rt = 2 dB, and $K = 0.5$. These results indicate that increasing m improves

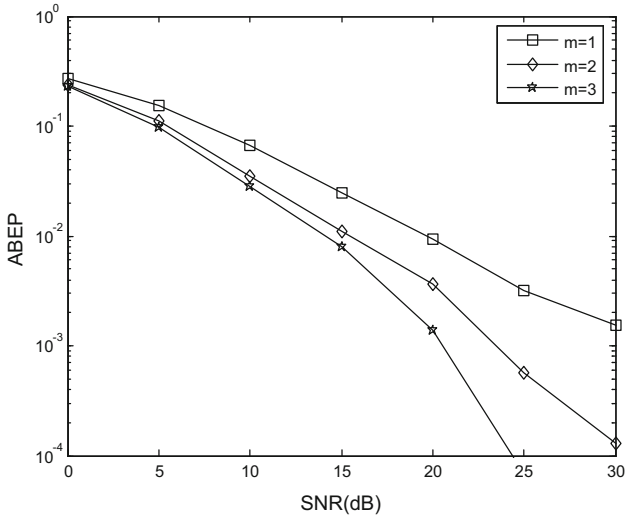

Fig. 9 The effect of m on the ABEP performance

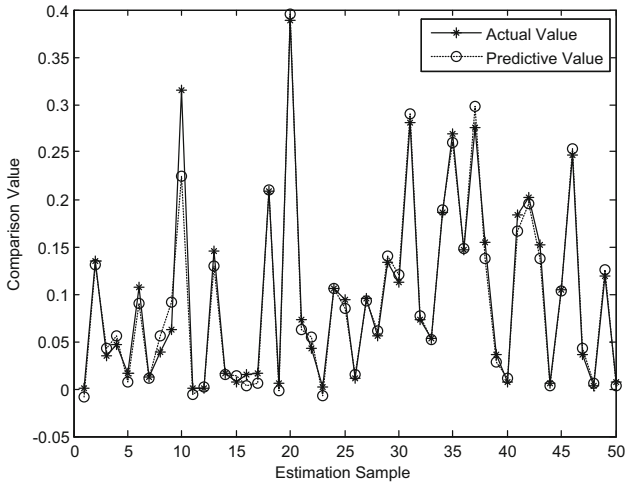

Fig. 10 Actual and predicted BP neural network outputs

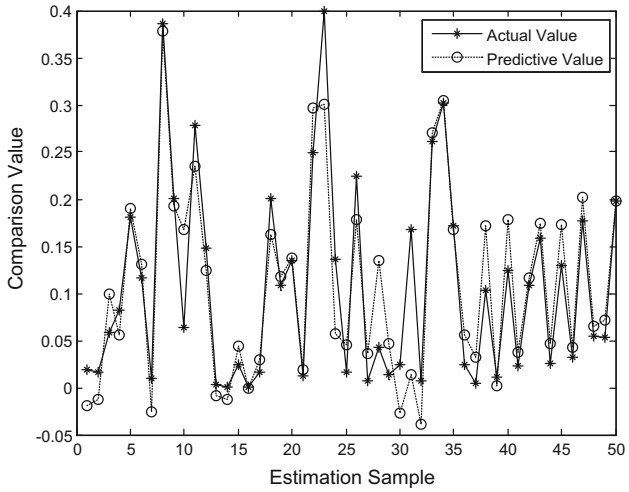

Fig. 11 Actual and predicted ELM outputs

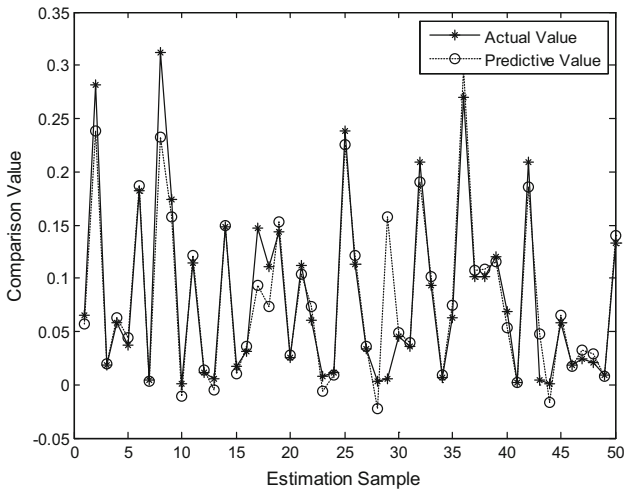

Fig. 12 Actual and predicted SVM outputs

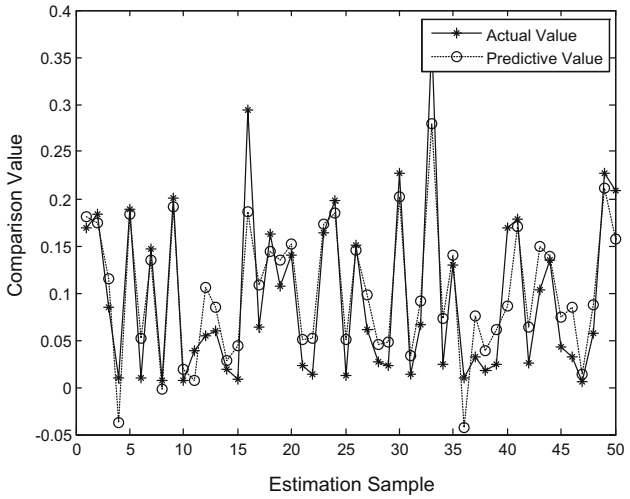

Fig. 13 Actual and predicted LR outputs

Table 3 The parameters for four methods

Algorithm	BP	ELM	SVM	LR
Number of training sets:950 Number of test sets: 50				
X	11	11	11	11
y	y:1	1	1	1
	q:10	*q*:2559	*c*: 11.314	tau:0.49
	a:0.1		*g*: 0.03125	

Table 4 The running time and MSE for four methods

Algorithm	BP	ELM	SVM	LR
Running Time	3.31 s	2.36 s	75.67 s	5.60 s
MSE	0.00026	0.0019	0.00085	0.0016

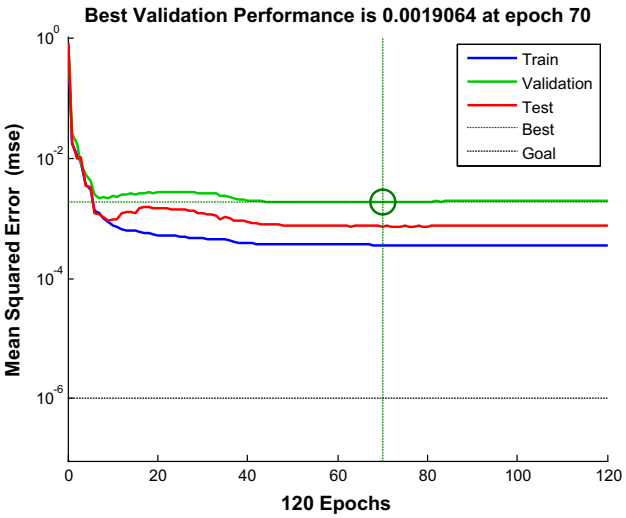

Fig. 14 Validation performance of BP neural network

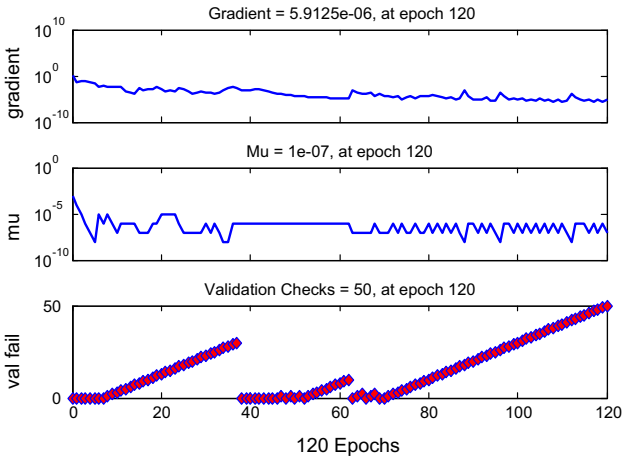

Fig. 15 Training state of the BP neural network

the ABEP. When SNR = 15 dB, the ABEP is 2.8×10^{-2} for $m = 1$, 1×10^{-2} for $m = 2$, and 8×10^{-3} for $m = 3$.

Figures 10, 11, 12, and 13 compare the performance of the BP neural network with the LR [38], SVM [39], and ELM [40] methods. The parameters for the four methods are given in Table 3. These results show that the MSE of the BP neural network is 0.00026, which is lower than that of the LR, SVM, and ELM methods, and indicate that the proposed method can consistently achieve higher ABEP performance prediction results.

Table 4 gives the running time and MSE for the four methods. This shows that, compared to ELM, BP has a longer running time, but the performance is better than with ELM. Also, compared to SVM and LR, BP has a shorter running time and smaller MSE. In conclusion, BP is the best forecasting model.

Figure 14 illustrates the validation performance. This shows that the MSE generally improves as the number of

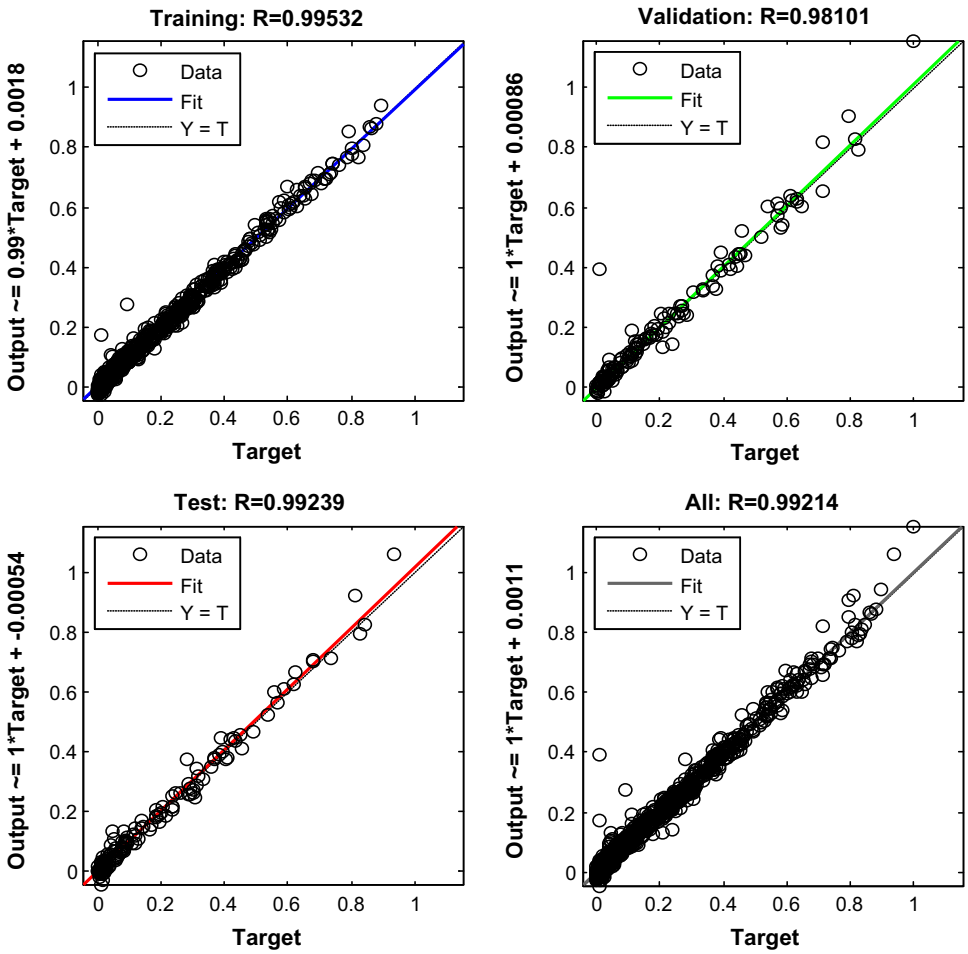

Fig. 16 Regression results for the BP neural network

Table 5 The effect of the number of neurons in the hidden layer on the MSE

Number of neurons	MSE
4	0.000838
5	0.000651
6	0.000548
7	0.000506
8	0.000497
9	0.000481
10	0.000260
11	0.000315
12	0.000306
13	0.000399
14	0.000484

epochs increases. In our setup, if the validation error increases for 50 consecutive epochs, the training stops. In the figure, this occurs after 120 epochs while the best validation performance is 0.0019064 at epoch 70.

In Fig. 15, we can obtain the training state. In training state, the BP uses gradient descent method. From Fig. 15, we can see how the gradient change as the number of epochs increases. From the 70 epoch, the validation error increases. After 50 consecutive increasing at the 120 epoch, the validation checks fail 50 times and the training state will stop.

The regression results are shown in Fig. 16. The relationship between the targets and outputs is indicated by the correlation coefficient R. A larger R means the BP neural network model has better prediction capability. In Fig. 16, R is 0.99214, which indicates that the proposed method has good prediction capability.

Table 5 gives the effect of the number of neurons in the hidden layer on the MSE. This shows that when the number of neurons is small, the MSE performance is poor. The MSE performance improves as the number of neurons increases. However, with a sufficiently large number of neurons, the structure of the neural network is too complex and the MSE begins to decrease. In the proposed networks the best MSE performance is achieved when there are 10 neurons.

The training function employed also affects the MSE performance. Table 6 shows the effect of six different

Table 6 The effect of different training functions on the MSE

Training function	Abbreviation	MSE
Levenberg–Marquardt	trainlm	0.000260
Fletcher–Reeves	traincgf	0.000362
Gradient descent	traingd	0.003010
Gradient descent with adaptive learning rate	traingda	0.001200
Gradient descent with momentum	traingdm	0.003800
Gradient descent with momentum and adaptive learning rate	traingdx	0.000482

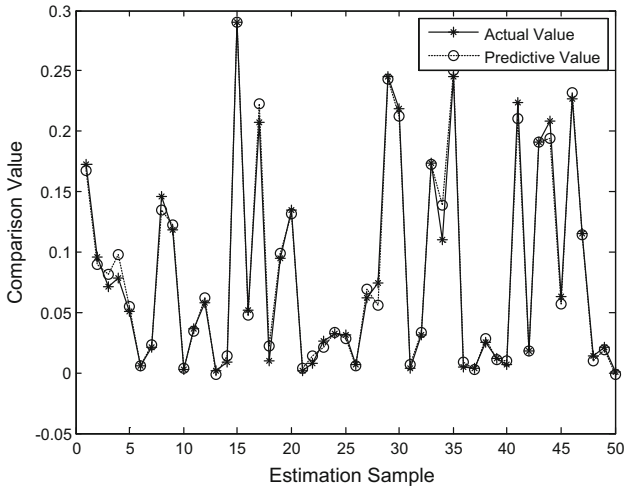

Fig. 17 Actual and predicted outputs of a network with two hidden-layers

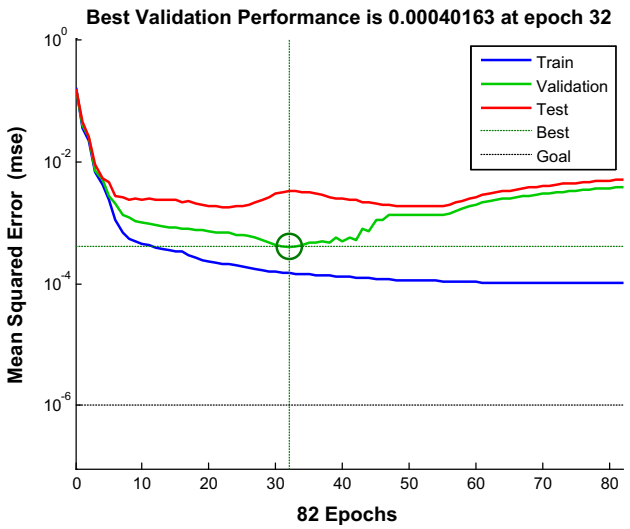

Fig. 18 Validation performance of a network with two hidden layers

training functions on the MSE. This indicates that the best training function is the Levenberg–Marquardt function with an MSE of 0.000260.

We also considered the effect of the number of hidden layers on the MSE performance. Figures 17, 18, 19, and 20, show the MSE performance, validation performance,

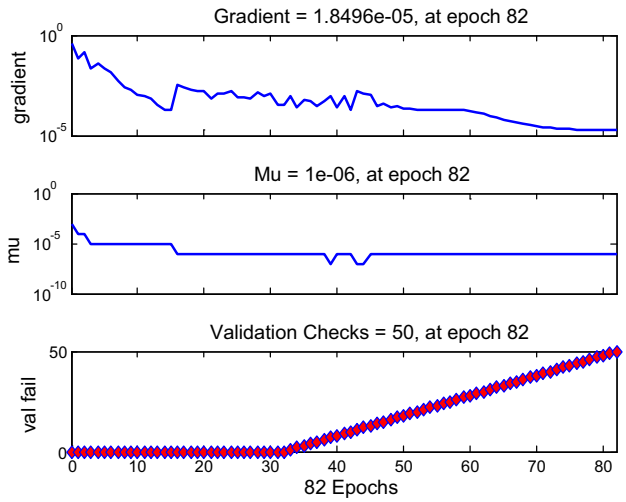

Fig. 19 Training state of a network with two hidden layers

training state, and regression for a network with two hidden layers.

Table 7 shows the effect of different numbers of hidden layers on the MSE performance. The performance with two hidden layers is better than that with one hidden layer, but the running time with two hidden-layers is longer. Thus, increasing the number of layers can improve the MSE performance, but will also increases the running time.

8 Conclusion

Closed-form PDF and CDF expressions for the direct link SNR and end-to-end link SNR were derived for a mobile cooperative communication system. These results were used to derive an exact closed-form ABEP expression. A BP neural network-based ABEP performance prediction algorithm was proposed. To verify the analysis, theoretical results were compared with Monte-Carlo simulation results. In addition, these results indicated that m, N, μ, and K can significantly affect the ABEP performance. As m is increased and N and μ are reduced, the ABEP performance is improved. Compared to the LR, SVM, and ELM methods, the experimental results verify that the proposed method can consistently achieve higher ABEP performance prediction results.

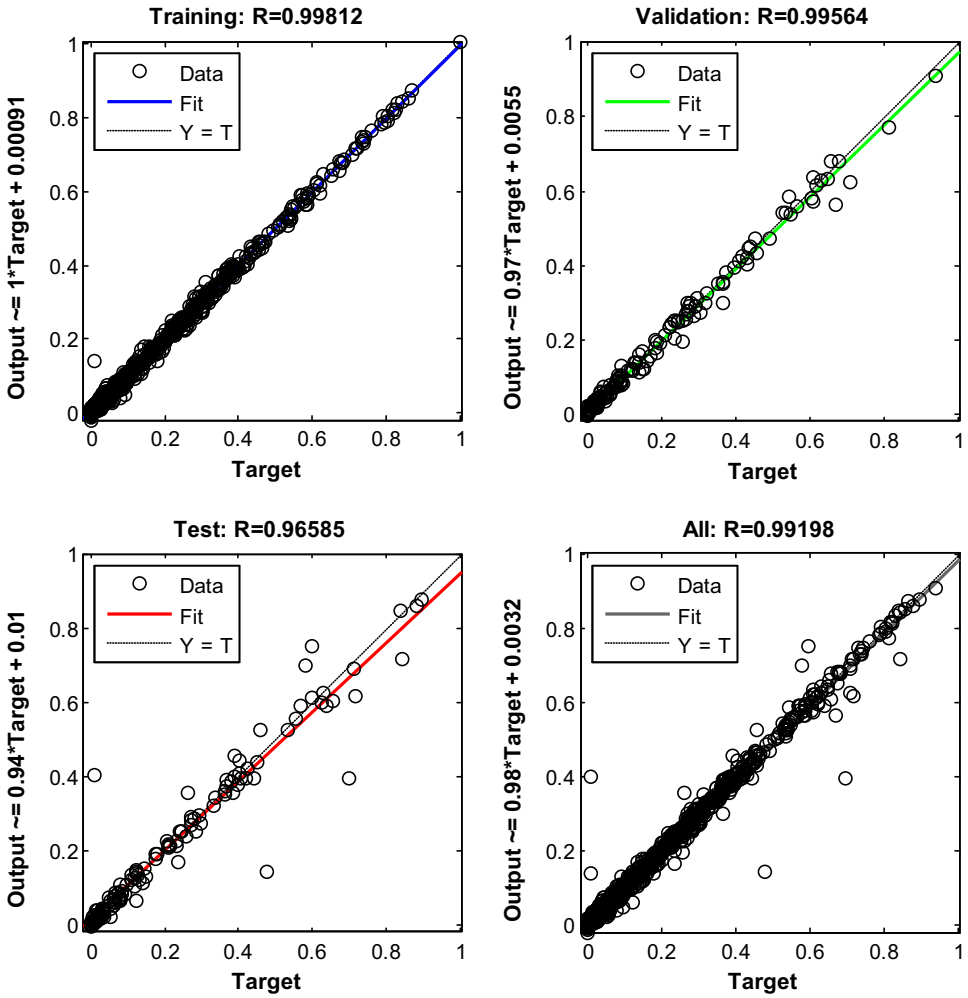

Fig. 20 Regression results for a network with two hidden layers

Table 7 The effect of the number of hidden layers on the MSE

	1 hidden layer	2 hidden layers
MSE	2.60e−04	6.29e−05
Time	3.313 s	3.9109125 s

Acknowledgements This research was supported by the National Natural Science Foundation of China (Nos. U1806201, 61671261, 61901409), the Shandong Province Colleges and Universities Young Talents Initiation Program (No. 2019KJN047), the Opening Foundation of Key Laboratory of Opto-technology and Intelligent Control (Lanzhou Jiaotong University), the Ministry of Education (Grant No. KFKT2018-2), the Shandong Province Natural Science Foundation (No. ZR2017BF023), the Shandong Province Postdoctoral Innovation Project (No. 201703032), and the Doctoral Fund of QUST (No. 010029029).

Compliance with ethical standards

Conflict of interest The authors declare that they have no conflict of interest.

References

1. Wang D, Chen D, Song B, Guizani N, Yu XY, Du XJ (2018) From IoT to 5G I-IoT: the next generation IoT-based intelligent algorithms and 5G technologies. IEEE Commun Mag 56(10):114–120
2. Bedi G, Venayagamoorthy GK, Singh R, Brooks RR, Wang KC (2018) Review of internet of things (IoT) in electric power and energy systems. IEEE Internet of Things Journal 5(2):847–870
3. Hou XM, Zhang FQ, Liu D (2017) Dynamic coordination process based on predictive graph in mobile cloud environment. J Liaocheng Univ (Nat Sci Ed) 30(4):96–100
4. Xu LW, Wang JJ, Zhang H, Gulliver TA (2017) Performance analysis of IAF relaying mobile D2D cooperative networks. J Frankl Inst 354(2):902–916
5. Li JQ (2018) Solving reverse logistic problem in prefabricate system by a discrete artificial bee colony algorithm. J Liaocheng Univ (Nat Sci Ed) 31(2):102–110
6. Zhou SY, Liu X, Effenberger F, Chao J (2018) Low-latency high-efficiency mobile fronthaul with TDM-PON (mobile-PON). IEEE/OSA J Opt Commun Networking 10(1):A20–A26
7. Li Y, Sun K, Cai L (2018) Cooperative device-to-device communication with network coding for machine type communication devices. IEEE Trans Wireless Commun 17(1):296–309
8. Li XW, Liu M, Deng C, Mathiopoulos PT, Ding ZG, Liu YW (2019) Full-duplex cooperative NOMA relaying systems with I/Q

imbalance and imperfect SIC. IEEE Wirel Commun Lett. https://doi.org/10.1109/LWC.2019.2939309
9. Lin ME (2016) Computer network attack modeling method based on attack graph. J Liaocheng Univ (Nat Sci Ed) 29(3):100–104
10. Lei HJ, Yang ZX, Park KH, Ansari IS, Guo YC, Pan GF, Alouini MS (2019) Secrecy outage analysis for cooperative NOMA systems with relay selection schemes. IEEE Trans Commun 67(9):6282–6298
11. Lei HJ, Zhang ZM, Park KH, Xu P, Zhang ZF, Pan GF, Alouini MS (2018) Secrecy outage of max-min TAS scheme in MIMO-NOMA systems. IEEE Trans Veh Technol 67(8):6981–6990
12. Wang HM (2017) Full-Diversity uncoordinated cooperative transmission for asynchronous relay networks. IEEE Trans Veh Technol 66(1):468–480
13. El-Malek AHA, Salhab AM, Zummo SA (2017) New bandwidth efficient relaying schemes in cooperative cognitive two-way relay networks with physical layer security. IEEE Trans Veh Technol 66(6):5372–5386
14. Mahmood NH, Ansari IS, Popovski P, Mogensen P, Qaraqe KA (2017) Physical-layer security with full-duplex transceivers and multiuser receiver at Eve. IEEE Trans Commun 65(10):4392–4405
15. İlhan H, Uysal M, Altunbas I (2009) Cooperative diversity for intervehicular communication: performance analysis and optimization. IEEE Trans Veh Technol 58(7):3301–3310
16. Yu JS, Bi MH, Zhuo XH, Huang TC (2018) IMDD-UMFC system performance improvement based on non-uniform quantization ADC/DAC. Journal of Liaocheng University (Natural Science Edition) 31(4):7–12
17. Nguyen BC, Hoang TM, Dung LT (2019) Performance analysis of vehicle-to-vehicle communication with full-duplex amplify-and-forward relay over double-Rayleigh fading channels. Vehic Commun 19:100166
18. Nguyen SQ, Kong HY (2016) Outage probability analysis in dual-hop vehicular networks with the assistance of multiple access points and vehicle nodes. Wirel Pers Commun 87(4):1175–1190
19. Ai Y, Cheffena M, Mathur A, Lei HJ (2018) On physical layer security of double Rayleigh fading channels for vehicular communications. IEEE Wirel Commun Lett 7(6):1038–1041
20. Pandey A, Yadav S (2018) Physical layer security in cooperative AF relaying networks with direct links over mixed Rayleigh and double-Rayleigh fading channels. IEEE Trans Veh Technol 67(11):10615–10630
21. Alghorani Y, Kaddoum G, Muhaidat S, Pierre S, Al-Dhahir N (2016) On the performance of multihop-intervehicular communications systems over *n**Rayleigh fading channels. IEEE Wirel Commun Lett 5(2):116–119
22. Nguyen BC, Tran XN, Hoang TM, Dung LT (2019) Performance analysis of full-duplex vehicle-to-vehicle relay system over double-Rayleigh fading channels. Mob Networks Appl. https://doi.org/10.1007/s11036-019-01291-x
23. Wang H, Xu LW, Lin WZ, Xiao PP, Wen R (2019) Physical layer security performance of wireless mobile sensor networks in smart city. IEEE Access 7:15436–15443
24. Karagiannidis GK, Sagias NC, Mathiopoulos PT (2007) *N**Nakagami: a novel stochastic model for cascaded fading channels. IEEE Trans Commun 55(8):1453–1458
25. Xu LW, Wang JJ, Zhang H, Liu Y, Shi W, Gulliver TA (2018) Outage performance for IDF relaying mobile cooperative networks. Mobile Networks & Applications 23(6):1496–1501
26. Xu LW, Yu X, Wang H, Dong XL, Liu Y, Lin WZ, Wang XJ, Wang JJ (2019) Physical layer security performance of mobile vehicular networks. Mob Netw Appl. https://doi.org/10.1007/s11036-019-01224-8
27. Zhang WP, Kumar M, Liu JQ (2019) Multi-parameter online measurement IoT system based on BP neural network algorithm. Neur Comput Appl 31(12):8147–8155
28. Hu ZL, Zhao Q, Wang J (2018) The prediction model of cotton yarn intensity based on the CNN-BP neural network. Wireless Pers Commun 102(2):1905–1916
29. Xu LW, Wang H, Lin W, Gulliver TA, Le Khoa N (2019) GWO-BP neural network based OP performance prediction for mobile multiuser communication networks. IEEE Access 7:152690–152700
30. Yu RY, An XM, Jin B, Shi J, Move OA, Liu YH (2018) Particle classification optimization-based BP network for telecommunication customer churn prediction. Neural Computing & Application 29(3):707–720
31. Liu X, Zhou YJ, Wang ZR, Chen XH (2018) A BP neural network-based communication blind signal detection method with cyber-physical-social systems. IEEE Access 6:43920–43935
32. Liu L (2019) Recognition and analysis of motor imagery EEG signal based on improved BP neural network. IEEE Access 7:47794–47803
33. Li ZX, Jia LZ, Li F, Hu HY (2010) Outage performance analysis in relay-assisted inter-vehicular communications over double-Rayleigh fading channels. In: Proceedings of the IEEE International Conference on Communications and Mobile Computing, Shenzhen, China, pp 266–270
34. Hasna MO, Alouini MS (2004) Harmonic mean and end-to-end performance of transmission systems with relays. IEEE Trans Wireless Commun 52(1):130–135
35. Anghel PA, Kaveh M (2004) Exact symbol error probability of a cooperative network in a Rayleigh-fading environment. IEEE Trans Wireless Commun 3(5):1416–1421
36. Gradshteyn I, Ryzhik I (2007) Table of Integrals, Series and Products, 7th edn. Academic Press, San Diego
37. The Wolfram Functions Site (Online). http://functions.wolfram.com/. Accessed Feb 22 2018
38. Cola TD, Mongelli M (2018) Adaptive time window linear regression for outage prediction in Q/V band satellite systems. IEEE Wireless Communications Letters 7(5):808–811
39. Yu X, Chu Y, Jiang F, Guo Y, Gong DW (2018) SVMs classification based two-side cross domain collaborative filtering by inferring intrinsic user and item features. Knowl-Based Syst 141:80–91
40. Xu KK, Yang HD, Zhu CJ (2019) A novel extreme learning machine-based Hammerstein-Wiener model for complex nonlinear industrial processes. Neurocomputing 358(9):246–254